T H E U N I V E R S I T Y O F M I C H I G A N

COLLEGE OF LITERATURE, SCIENCE, AND THE ARTS
Department of Physics

Progress Report

THE UNIVERSITY OF MICHIGAN 42-INCH CYCLOTRON

W. C. Parkinson
Professor of Physics

R. S. Tickle
Assistant Professor of Physics

ORA Project 2842

under contract with:

UNITED STATES ATOMIC ENERGY COMMISSION
CHICAGO OPERATIONS OFFICE
CONTRACT NO. AT(11-1)-275
ARGONNE, ILLINOIS

administered through:

OFFICE OF RESEARCH ADMINISTRATION ANN ARBOR

July 1961

TABLE OF CONTENTS

PERSONNEL

Faculty

W. C. Parkinson

R. S. Tickle

Research Associates

C. Daum

T. Holtebekk

J. Jänecke

Graduate Students

J. Bardwick III
D. Donnelly
J. A. Green

G. Knoll*
J. R. Maxwell
F. Sevcik

Technical Staff

W. E. Downer

J. A. Koenig

R. D. Pittman

Plate Readers

J. A. Desai
E. S. Foerg
L. L. Graf
F. M. Hilberger
A. E. Klumpp

R. T. Rao
G. Sanders
L. Shanklin
B. B. Stark
S. C. Tomlinson

*Nuclear Engineering

ABSTRACT

This report describes the experimental and theoretical research effort of the Michigan 42-inch cyclotron group during the period from July, 1960, to July, 1961. The several problems which received major attention are: level-structure studies of the (ld,2s) shell nuclei Na^{24}, Mg^{25}, Mg^{26}, Mg^{27}, $A\ell^{28}$, P^{32}, S^{33}, S^{35}, $C\ell^{36}$, $C\ell^{38}$; deuteron elastic scattering from several nuclei; proton polarization in the $Be^{9}(d,p)Be^{10}$ reaction; the neutron time-of-flight spectrometer; and solid-state particle detectors.

I. INTRODUCTION

During the period covered by this report the principal effort of the cyclotron group was devoted to the experimental study of (1d,2s) shell nuclei and to the interpretation of the results in terms of the collective model. While most of the cyclotron running time was spent on this general problem, work continued on the problems of polarization in stripping, the neutron-time-of flight spectrometer, and solid-state detectors.

In contrast to the difficulties reported last year, relatively few days were lost in cyclotron operation. A total of 2,800 hours of actual "beam on target" time was recorded, or an average of nearly eight hours every day of the 365 days of the year. Some 100 hours were spent in routine maintenance and approximately 120 hours in unscheduled maintenance and repair.

Approximately 40 hours were spent showing some 800 visitors through the facility.

More that 2,600 1 x 10-in. nuclear track plates have been exposed and developed since the last report. The nuclear emulsion scanner continued to operate satisfactorily within its inherent limitations and approximately 560 plates were scanned with it. The great majority of plates, however, namely, 2,300, were read by human scanners. Some 1,800 girl-days were spent in extracting and plotting the data. Because of the limited number of microscopes available, the scanners have been working in two shifts for the last half year.

II. THE EXPERIMENTAL PROGRAM

Sections A through I below describe the research effort directed toward determining how well, in view of the success with Mg^{25}, the collective model can account for the experimental data of other (1d,2s) shell nuclei. The results indicate that while many of the qualitative features are correctly predicted by the model, the amount of data presently available is far too limited to obtain a definitive answer. One fact, however, does emerge clearly from this work; no real progress can be made in the theoretical interpretation until our knowledge of the spins, moments, and transition probabilities is greatly increased. Parities and reduced widths, while important, do not provide sufficient data.

The experimental group has devoted considerable effort this past year to the theoretical understanding of the problems of nuclear structure from the point of view of both the shell model and the collective model of the nucleus. In this effort we have been helped immeasurably by K. T. Hecht, who in addition to giving a brilliant series of lectures this past year on nuclear models, has worked individually with members of the experimental group on the interpretation of their data. Many of the calculations described in this report would not have been performed without his assistance.

A. THE LEVEL STRUCTURE OF Na^{24}

Measurements of the $Na^{23}(d,p)Na^{24}$ reaction,[1] a preliminary report of which was given last year, have been essentially completed for the range of excitation up to 7 Mev. An additional measurement, the deuteron elastic scattering on Na^{23}, has been completed to determine the optical model parameters required for distorted wave calculations of the stripping angular distributions.

Two of the levels reported last year have been shown to arise from contamination of F^{19} in the target leading to the $F^{19}(d,p)F^{20}$ reaction. The contamination was mainly due to the Teflon insulator of the Faraday-cup, and the fact that the target material has a high affinity for flourine. The Teflon has since been replaced by a lava insulator. A small amount of F^{19} is still present, however, due to the Teflon insulators on the dee stems and on the extractor of the cyclotron, and the strong $\ell_n = 2$ transition to the 2.048-Mev level in F^{20} covers in part the angular distribution of the transition to the 2.464-Mev level in Na^{24}. The 2.464-Mev level is characterized by $\ell_n = 1$ and has a strength of only 5-10% of the $\ell_n = 1$ transition to the next odd-parity level in Na^{24} at 3.37 Mev.

---

1. C. Daum, Bul. Am. Phys. Soc. II 6, 259 (KAI) (1961).

Figure 1 shows the 30° spectrum of Na^{24} obtained with a deuteron energy of 7.8 Mev. The width of the peaks is of the order of 25 kev. The results obtained for levels up to 5-Mev excitation are given in Table I. Previously unpublished levels have been found at 2.98-, 3.22-, 3.37-, 3.97-, 4.62-, and 4.69-Mev excitation, while the levels at 3.850, 3.899, and 4.219 Mev reported by the group at MIT[2] have not been identified, although some recent measurements in this region are still to be evaluated. The levels at 4.44 and 4.95 Mev are in good agreement with those reported by the Liverpool group.[3] The levels at 2.98, 3.37 and 4.53 Mev have also been found by the Los Alamos group[4] using the reaction $Na^{23}(n,\gamma)Na^{24}$, and agree with this work in assigning an excitation energy of 2.52 Mev to the level reported at 2.561 Mev by MIT.

Typical angular distributions are shown in Fig. 2, where Butler curves have been fitted for the major component of each angular distribution. Two features of these distributions are of particular interest. The ground state distribution is mainly $\ell_n = 2$. Since the ground state spin of Na^{24} is known to be 4^+ from β-decay, whereas the spin of Na^{23} is $3/2^+$, $\ell_n = 0$ is excluded on the basis of conservation of angular momentum. The weak forward peaking observed when $\ell_n = 0$ is forbidden, is characteristic of distorted wave effects.[5] The isomeric 0.472-Mev level is known to have a spin 1^+ from β-decay from Ne^{24}, so that both $\ell_n = 0$ and $\ell_n = 2$ are possible and the forward peaking is more pronounced. The apparent narrowness of the $\ell_n = 0$ peak is believed due to an instrumental effect and this point is being investigated. Distributions other than $\ell_n = 0$ behave normally, and all distributions appear to show the general pattern obtained with distorted wave calculations.

The relative reduced widths were calculated using Lubitz's tables[6] and are normalized to $\theta^2 = 1$ for the ground state. The spins of the first four levels are known form β-decay and from the (d,p) reaction. It is to be hoped that the measurements at Los Alamos, together with the results obtained here, will permit determination of the spins of many more levels.

The interpretation of the level scheme of Na^{24} containing 3 protons and 5 neutrons outside the doubly closed O^{16} core is not feasible on the basis of the shell model. The collective model, on the other hand, has been applied with reasonable success to Mg^{25} and Al^{25}, and it is of interest to consider the in-

---

2. A. Sperduto and W. W. Buechner, Phys. Rev. 88, 575 (1952).

3. A. W. Dalton, G. Parry, and M. D. Scott, private communication; F.A. El Bedewi and M. A. El Wahab, Nuclear Phys. 21, 69 (1960).

4. H. T. Motz, Los Alamos, private communication.

5. R. Satchler, Oak Ridge, private communication.

6. C. R. Lubitz, unpublished report, Department of Physics, University of Michigan.

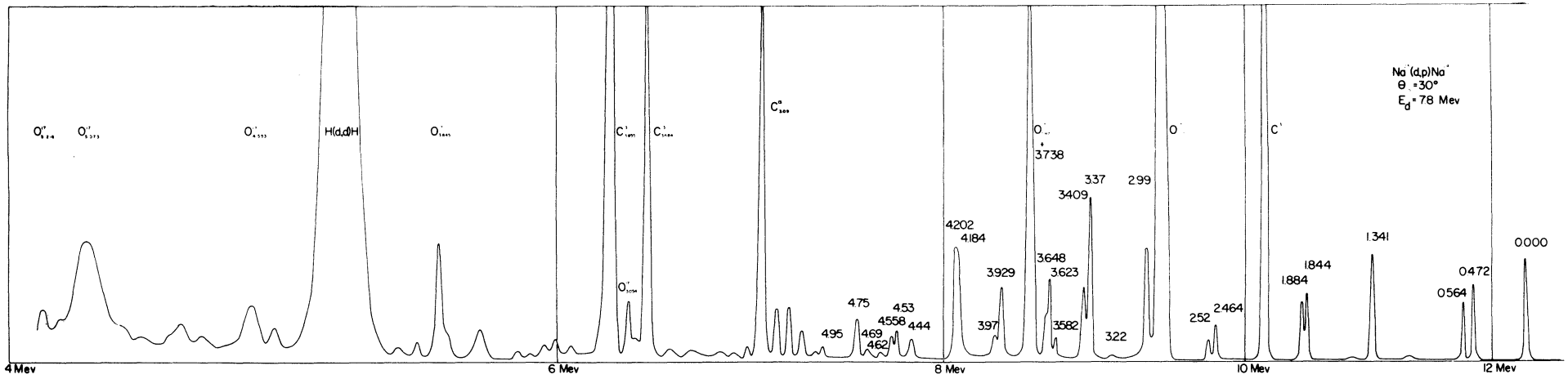
H(d,d)H
4 Mev
6 Mev
8 Mev
10 Mev
12 Mev
Na(d,p)Na
θ =30°
Ed = 78 Mev
4202
4184
3929
3738
3648
3623
3582
3409
337
322
299
252
2464
1884
1844
1341
0564
0472
0000
495
475
469
462
453
4558
444
397

Fig. 1

TABLE I

LEVELS IN Na^{24} FROM THE REACTION $Na^{23}(d,p)Na^{24}$

Q_o = 4.731 Mev; E_d = 7.77 Mev

Excitation Energy*	ℓ_n	Relative $(2J+1)\theta^2$	J	Relative θ^2
0	2	9.0	4^+	1.0
0.472	2	5.9	1^+	2.0
0.564	0	2.2	2^+	0.44
1.341	0	7.5	1^+	2.5
1.844	0	6.2	-	-
1.884	2	4.4	-	-
2.464	1	0.3 - 0.7	-	-
2.52	2	1.5	-	-
2.98	2	7.1	-	-
3.22	4	5.3	-	-
3.37	1	6.9	-	-
3.409	0	11.2	-	-
3.582	0	3.4	-	-
3.623	2	4.1	-	-
3.648	(2)	(2.5)	-	-
3.738	(3)	(6.4)	-	-
3.929	1	1.4	-	-
3.97	(1)	0.4	-	-
4.184	(2)	(2.9)	-	-
4.202	1	2.5	-	-
4.44	1	0.7	-	-
4.53	1	1.1	-	-
4.558	(2)	(1.4)	-	-
4.62	1	0.4	-	-
4.69	1	0.6	-	-
4.75	1	2.6	-	-
4.95	0	0.6	-	-

*Energies given to three decimal places are values from MIT.[2] The values given to two decimal places are levels not previously reported and have an uncertainty of $\pm$ 0.02 Mev.

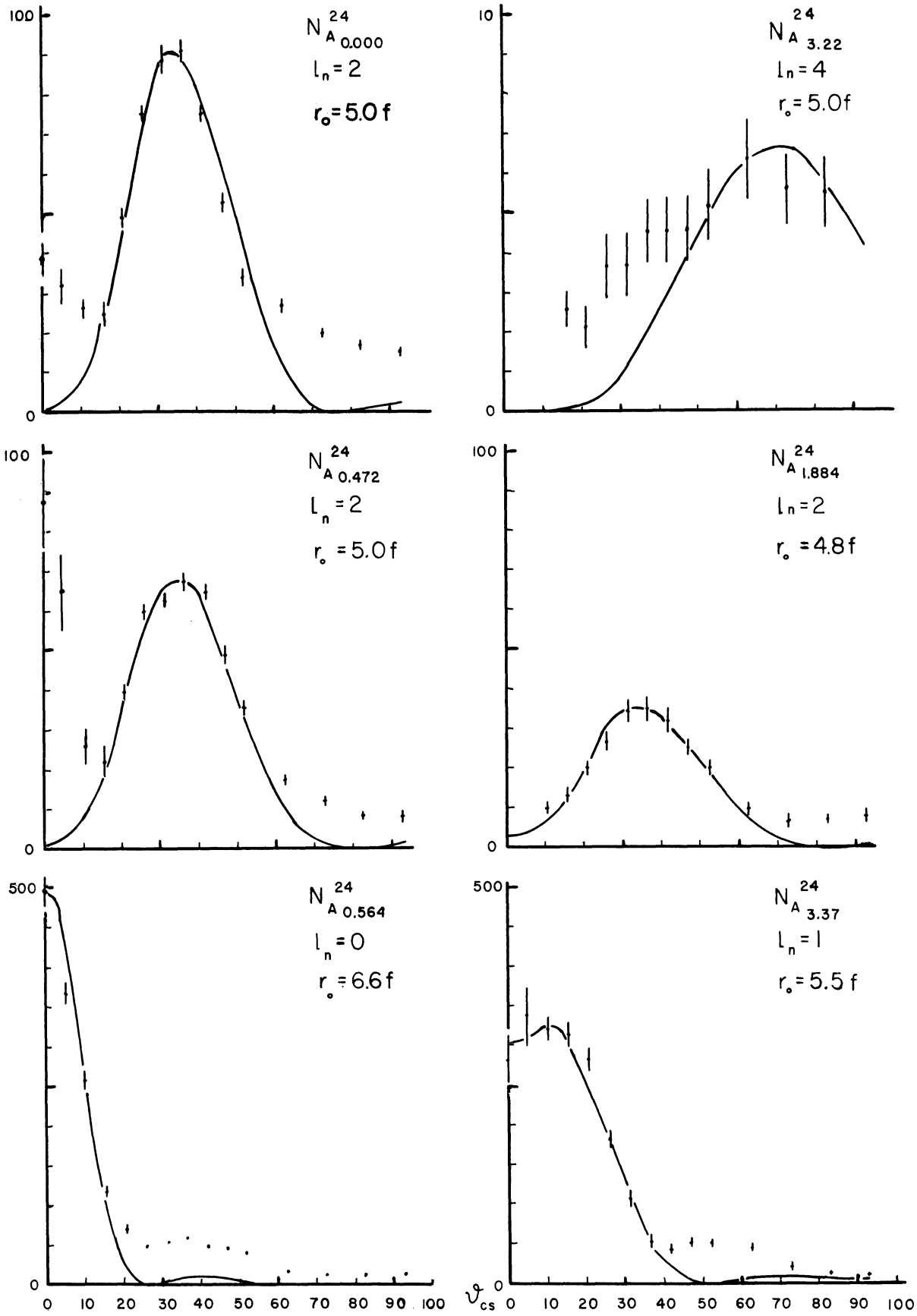
100
$N_{A\ 0.000}^{24}$
$l_n = 2$
$r_o = 5.0\,f$
0
10
$N_{A\ 3.22}^{24}$
$l_n = 4$
$r_o = 5.0f$
0
100
$N_{A\ 0.472}^{24}$
$l_n = 2$
$r_o = 5.0\,f$
0
100
$N_{A\ 1.884}^{24}$
$l_n = 2$
$r_o = 4.8f$
0
500
$N_{A\ 0.564}^{24}$
$l_n = 0$
$r_o = 6.6f$
0
500
$N_{A\ 3.37}^{24}$
$l_n = 1$
$r_o = 5.5\,f$
0
0 10 20 30 40 50 60 70 80 90 100
ϑ_{cs} 0 10 20 30 40 50 60 70 80 90 100

Fig. 2

terpretation of Na^{24} on the basis of this model. An additional complication arises, however, because Na^{24} is an odd-odd nucleus. In the terminology of the collective model there are two unpaired particles, one proton and one neutron, outside the core. The dipole moment of Na^{24} (1.69nm) suggests $\beta = +0.3$ which is consistent with the deformation $\beta = 0.3 - 0.4$ used in the interpretation of Na^{23}, Mg^{25}, and Al^{25}. For Na^{23}, in terms of the Nilsson diagram[7] shown in Fig. 3, levels through orbit #6 are filled while orbit #7 ($\Omega = 3/2$), contains two neutrons and one proton in agreement with the spin 3/2+ for the ground state of Na^{23}. The extra neutron in Na^{24} can therefore be captured in the even-parity levels #5 ($\Omega = 5/2$), #9 ($\Omega = 1/2$), #11 ($\Omega = 1/2$) and #8 ($\Omega = 3/2$) in the (1d,2s) shell, or in the odd-parity levels #14 ($\Omega = 1/2$), #13 ($\Omega = 3/2$), #12 ($\Omega = 5/2$) and #10 ($\Omega = 7/2$) in the (1f,2p) shell, etc. The assumption of a large deformation for Na^{24} is also consistent with the fact that the first odd-parity level at 2.464 Mev occurs at such low excitation. The relative weakness of the transition to this level compared to that of the 3.37-Mev level also is consistent with the predictions of the collective model, namely, that the admixture of p-state wave functions in the f-shell is small for the lowest odd-parity state.

A total of eight rotational bands can be expected to arise from the (1d,2s) shell alone, 4 with $K = \Omega = \Omega_p + \Omega_n$ and 4 with $K = \Omega = \Omega_p - \Omega_n$, where $\Omega_p = 3/2$ (level #7). In each case, however, there are numerous perturbations of the pure bands due to rotation-particle coupling (RPC) and many of these can be expected to be strong. Further, transitions to levels which involve multiple excitation are possible although these in general are much weaker and generally do not show clear stripping-type angular distributions. Thus a proper analysis should also take in account RPC with these levels as many of these matrix elements may not be negligible.

Results of preliminary computations, neglecting the interaction of levels due to multiple excitation, are encouraging. These computations are now being extended and further results should be available within the next year.

B. THE LEVEL STRUCTURE OF THE MAGNESIUM ISOTOPES

Study of the three isotopes of magnesium, $Mg^{25,26,27}$, by means of the (d,p) reaction has been continued.[8] The energy levels up to 6 Mev excitation have been determined and angular distributions obtained for them. The three spectra are compared in Fig. 4 which also includes the spectrum obtained for natural magnesium.

Some detailed remarks concerning Mg^{25} and Mg^{26} were given in the last report. The present discussion will be confined to the experimental results ob-

7. S. G. Nilsson, Dan. Mat. Fys. Medd. 29, No. 16 (1955).

8. W. C. Parkinson, Bul. Am. Phys. Soc. II 6, 259 (KA2) (1961).

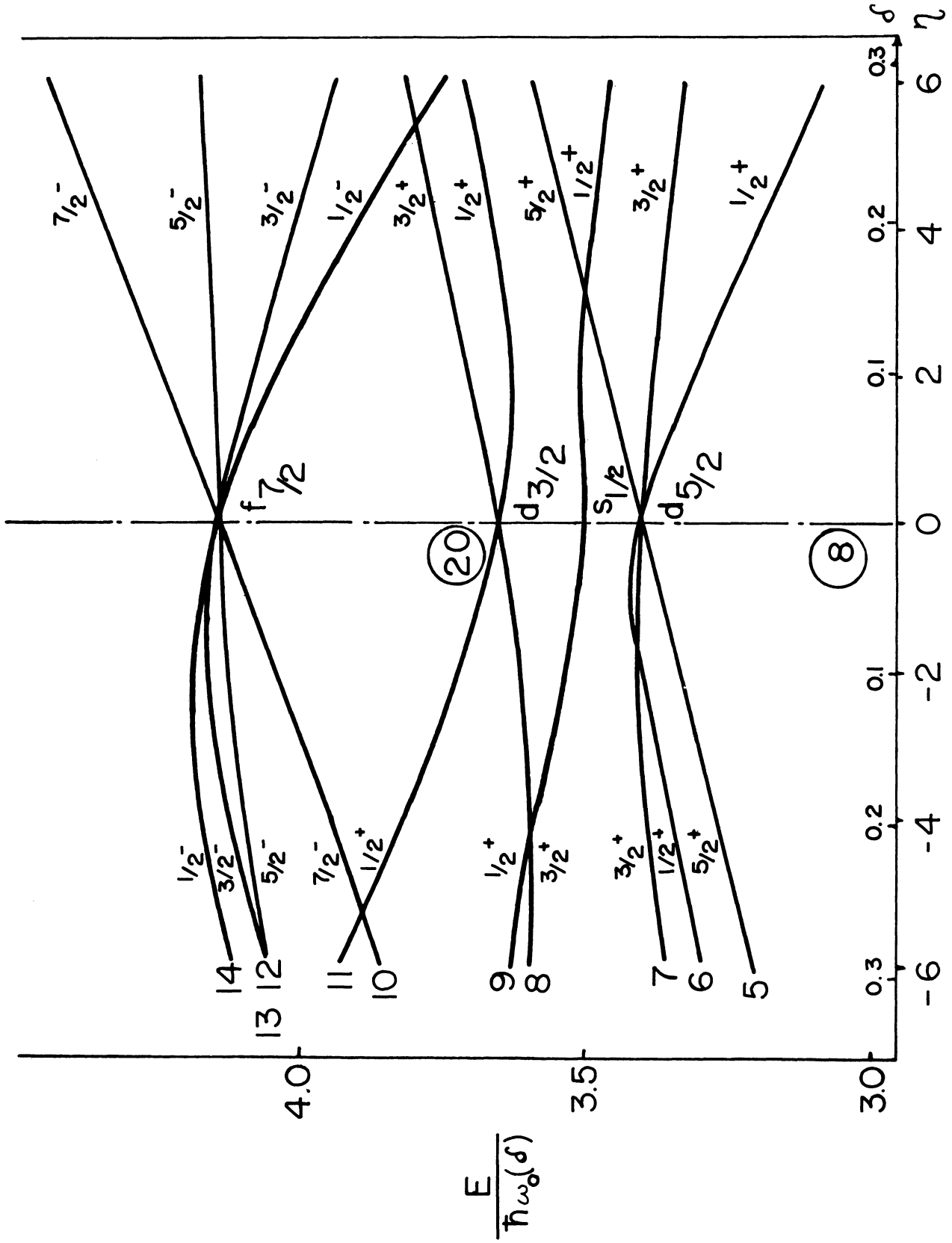
E / ħω₀(δ)
4.0
3.5
3.0
δ
η
0.3
0.2
0.1
0
0.1
0.2
0.3
6
4
2
0
-2
-4
-6
f7/2
d3/2
s1/2
d5/2
20
8
7/2⁻
5/2⁻
3/2⁻
1/2⁻
3/2⁺
1/2⁺
5/2⁺
1/2⁺
3/2⁺
1/2⁺
1/2⁻
3/2⁻
5/2⁻
7/2⁻
1/2⁺
1/2⁺
3/2⁺
3/2⁺
1/2⁺
5/2⁺
14
12
13
11
10
9
8
7
6
5

Fig. 3

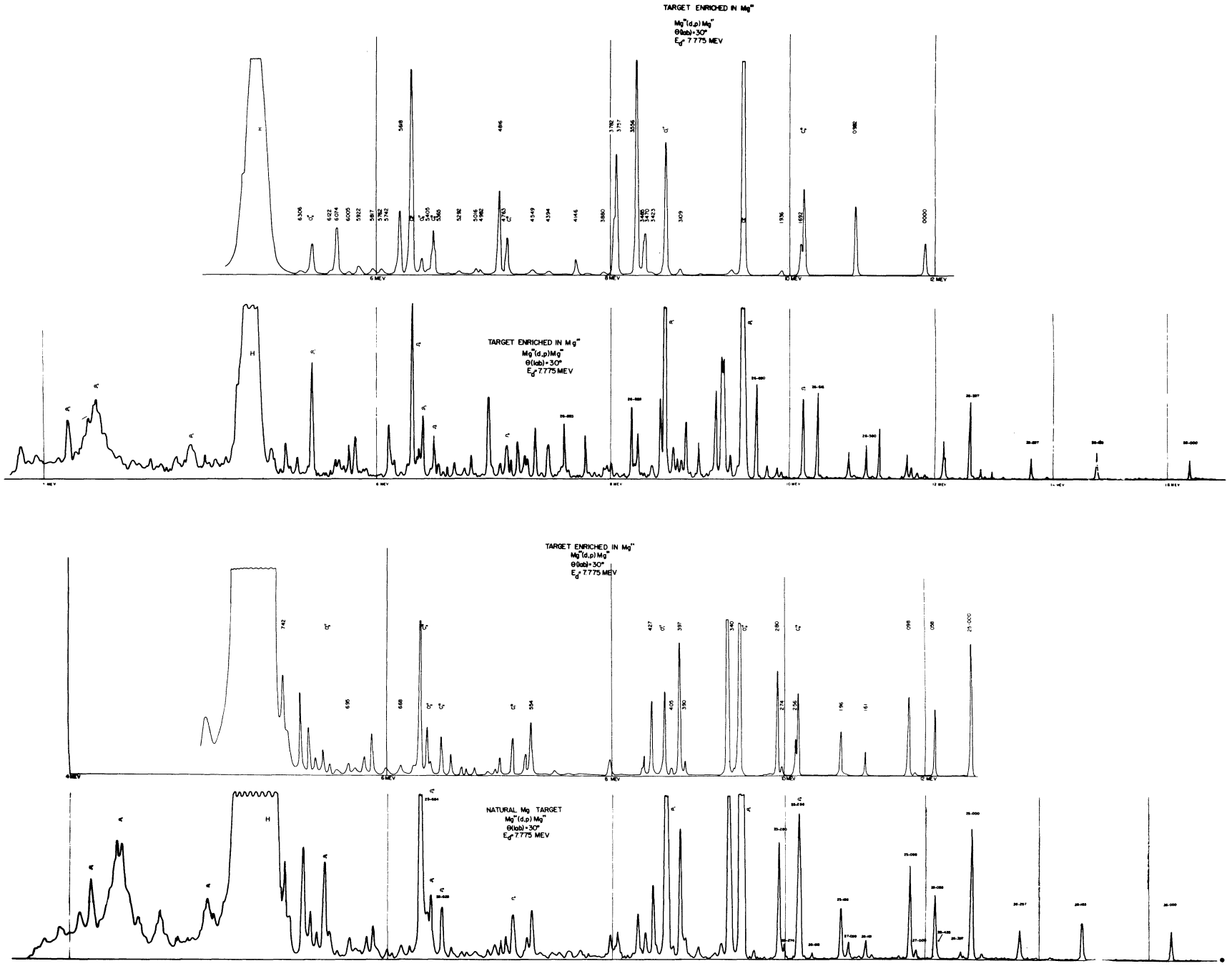
TARGET ENRICHED IN Mg²⁶
Mg²⁶(d,p) Mg²⁷
θ(lab)=30°
E_d=7.775 MEV
TARGET ENRICHED IN Mg²⁵
Mg²⁵(d,p)Mg²⁶
θ(lab)=30°
E_d=7.775 MEV
TARGET ENRICHED IN Mg²⁴
Mg²⁴(d,p) Mg²⁵
θ(lab)=30°
E_d=7.775 MEV
NATURAL Mg TARGET
Mg²⁴(d,p) Mg²⁵
θ(lab)=30°
E_d=7.775 MEV

Fig. 4

tained for Mg^{27}, an even-odd nucleus, and to the possible description of these results in terms of the rotational model.

A total of 32 levels have been identified in Mg^{27} below 6.3-Mev excitation and of these only 8 show characteristic stripping patterns. The relative reduced widths have been extracted for these 8 levels. A few typical angular distributions are shown in Fig. 5.

The only information available on Mg^{27} in addition to the present measurements comes from the β-decay of Mg^{27} to Al^{27}. No information is available on the magnetic or electric moments, nor are there data on the γ-decay schemes or branching ratios. Mg^{27} β-decays to two levels in Al^{27}, the 1.013-Mev and the 0.842-Mev levels, and both transitions have a log ft = 4.8. Using the Nilsson formalism and assuming Mg^{27} and Al^{27} to have the same deformation, the Chalk River group[9] computed the log ft values as a function of the nuclear deformation and found the deformation to be positive with $\beta \simeq 0.15$.

In terms of the Nilsson diagram of Fig. 3, the ground state of Mg^{27} with its 12 protons and 15 neutrons has the proton orbits filled up to and including orbit #7, the $\Omega = 3/2$ level of the $1d_{5/2}$ configuration, while the neutrons fill orbit #5 with the odd neutron in orbit #9, the $\Omega = 1/2$ level of the $(2s_{1/2})$ configuration. Strong excited states produced in the (d,p) reaction are expected to correspond to promoting this last neutron into higher orbits and to certain rotational levels based on these orbits. Many levels can be expected to arise due to multiple excitation, as for example elevating a neutron from the filled #5 orbit, or a proton from the filled #7 orbit; but all such levels should be weak as seen in the (d,p) reaction.

In the region of excitation up to 6 Mev there should be rotational bands of even parity built on orbit #9, K = 1/2+; on orbit #11, also K = 1/2+; orbit #8, K = 3/2+; and a band of odd-parity built on orbit #14, K = 1/2-. In the observed spectrum shown schematically on the right in Fig. 6 the ground state and the level at 3.470 Mev are formed by capture of neutrons with $\ell_n = 0$, hence their spins must be 1/2+ since Mg^{26} has spin 0+, and these are identified as the I = 1/2 members of the two K = 1/2+ bands of orbits #9 and #11. Candidates for the corresponding 3/2+ members are at 0.982 and 3.757 Mev, both $\ell_n = 2$ levels. The level at 6.07 Mev, formed by $\ell_n = 2$ capture is the first strong $\ell_n = 2$ above 3.757 Mev and is identified as the I = 3/2+ level of the K = 3/2+ band of orbit #8. The strong odd-parity level at 3.556 for which $\ell_n = 1$ is assigned to orbit #14.

Considering only the three even-parity bands, all three can mix due to rotation-particle coupling (RPC), the mixing occurring between bands 9 and 11; 8 and 9; and 8 and 11. The computation of the mixing therefore involves a 3 x 3 matrix. In carrying out the computation the deformation β and the rota-

9. Litherland et al., Can J. Phys. 36, 378 (1958).

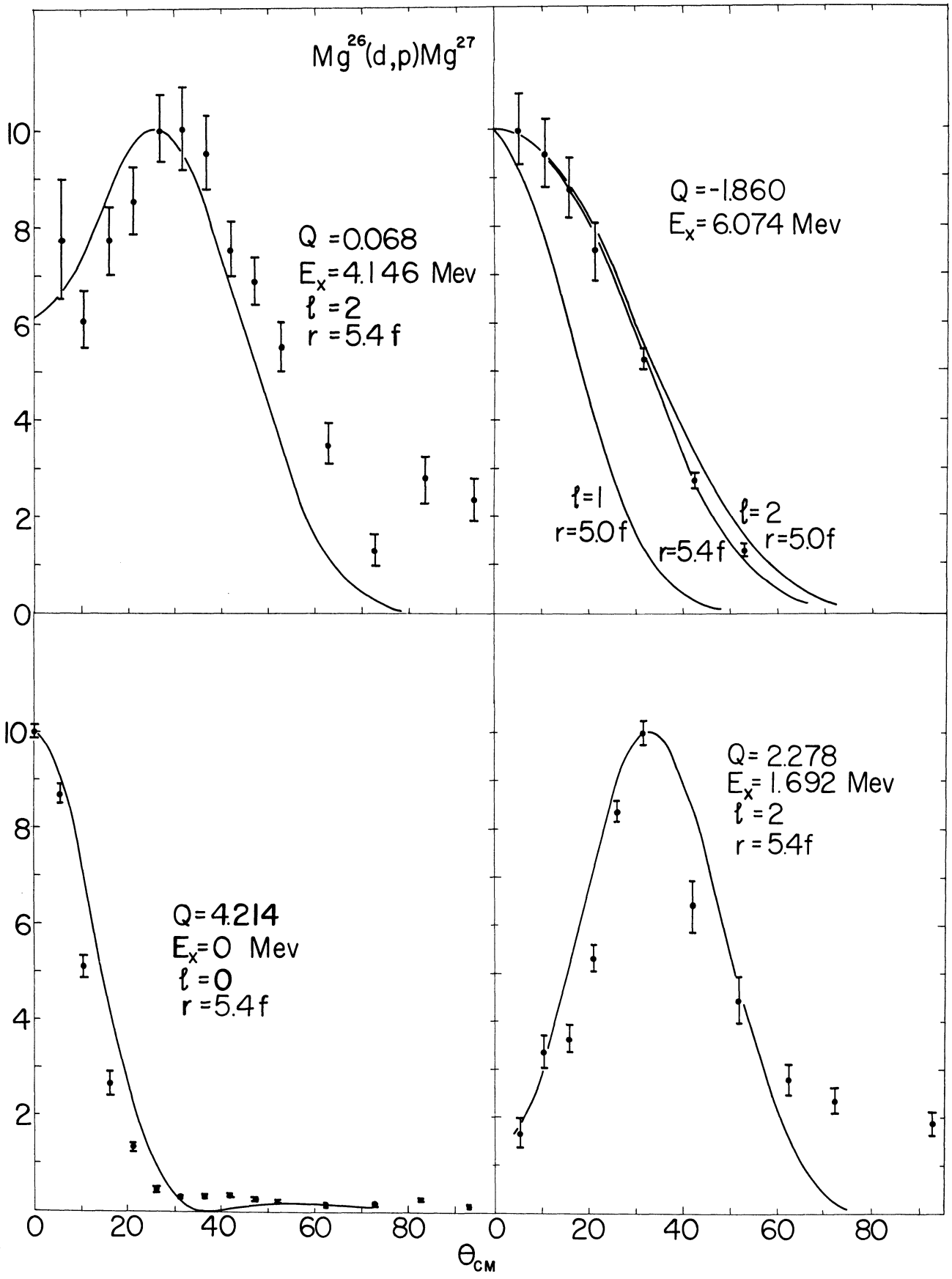
Mg26(d,p)Mg27
Q =0.068
Ex=4.146 Mev
ℓ =2
r =5.4 f
Q =-1.860
Ex= 6.074 Mev
ℓ=1
r=5.0f
r=5.4f
ℓ=2
r=5.0f
Q=4.214
Ex=0 Mev
ℓ =0
r =5.4f
Q= 2.278
Ex= 1.692 Mev
ℓ =2
r =5.4f
0
2
4
6
8
10
0
20
40
60
80
θcm

Fig. 5

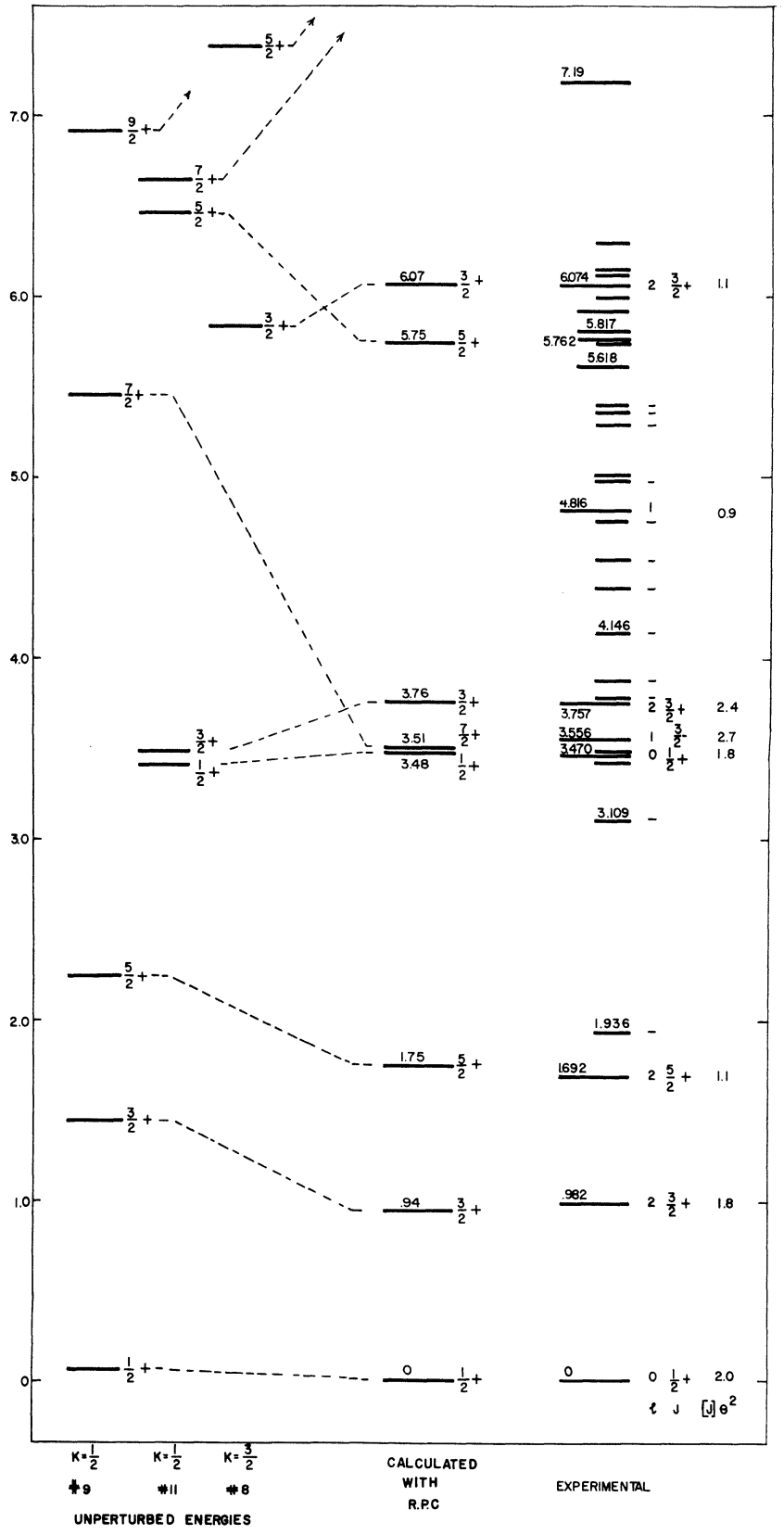
7.0
6.0
5.0
4.0
3.0
2.0
1.0
0
9/2+
7/2+
5/2+
5/2+
3/2+
7/2+
3/2+
1/2+
5/2+
3/2+
1/2+
6.07 3/2+
5.75 5/2+
3.76 3/2+
3.51 7/2+
3.48 1/2+
1.75 5/2+
.94 3/2+
0 1/2+
7.19
6.074
5.817
5.762
5.618
4.816
4.146
3.757
3.556
3.470
3.109
1.936
1692
.982
0
2 3/2+ 1.1
1 0.9
2 3/2+ 2.4
1 3/2- 2.7
0 1/2+ 1.8
2 5/2+ 1.1
2 3/2+ 1.8
0 1/2+ 2.0
ℓ J [J]θ²
K=1/2 #9
K=1/2 #11
K=3/2 #8
UNPERTURBED ENERGIES
CALCULATED WITH R.P.C
EXPERIMENTAL

Mg^{27}

Fig. 6

tional constant were varied to give the best fit to the 0.982-Mev (3/2+) and the 3.757-Mev (3/2+) levels. The values obtained are $\beta = +.16$ and $\hbar^2/2\mathcal{I} = 310$ kev. In attempting to fit the spectrum five parameters are required: three particle energies, β and $\hbar^2/2\mathcal{I}$. The spacings computed for the levels for each of the three bands neglecting RPC are shown on the left of Fig. 6. When RPC is included and all three bands mix the levels are pushed as shown by the dotted lines leading to the calculated energy diagram with RPC. Since five parameters are required, the only real check on the energy predictions comes from the 5/2+ levels at 1.692 and 5.76 Mev. This agreement is quite good since it must be remembered that a small change in a, the decoupling constant, can change the energies by the order of 10 kev, and that a rotation-vibration interaction, neglected here, as small as one kev can shift the energies of the higher spin levels by as much as 300-500 kev.

An example of a level believed due to multiple excitation occurs at 1.936 Mev. The excitation energy should be twice the $d_{5/2}$-$s_{1/2}$ separation, plus the difference in paring energy of two $d_{5/2}$ neutrons and two $s_{1/2}$ neutrons. The $d_{5/2}$-$s_{1/2}$ separation is of the order of 0.5-0.6 Mev so that a total excitation of 1.9 Mev is reasonable. Further, the level should have a spin of 5/2+ and be weak as seen in stripping. The 7/2+ level built on the 5/2+ band should occur, for the same constants used above, at 4.11 Mev. There is a candidate at 4.146 Mev, although the lower level at 3.880 is also a candidate.

An additional and critical test of the applicability of the model comes from the reduced widths. These are compared in Fig. 7. The measured values are indicated in the 4th column and are normalized to 2.0 for the ground state (2J+1). These values are to be compared first to the values calculated from the c_j^2 for the unperturbed system (col. 3) and to those calculated including RPC (col. 5). The agreement is surprisingly good for the unperturbed case except for the 6.07 level; further, applying the sum rule, the two K = 1/2 bands are very close indeed to the sum of the unperturbed reduced widths. Unfortunately, with RPC the agreement is less good, but still not unreasonable considering the uncertainties in extracting the reduced widths from the data. The one real improvement when RPC is included is in the reduced width for the 6.07-Mev level.

From the above results it can be concluded only that the observed energies and reduced widths are not inconsistent with the collective model, but more useful comparisons can only be made when the spins of many more levels are determined. Only then will it be useful to refine the calculations.

C. THE LEVEL STRUCTURE OF Al^{28}

The study of the level structure of the odd-odd nucleus Al^{28}, initiated last year, has been continued [10] using the Al^{27}(d,p) reaction. Angular dis-

10. R. S. Tickle and K. T. Hecht, Bul. Am. Phys. Soc. II 6, 259 (KA3) (1961).

REDUCED WIDTHS

	E(MEV)	J^{π}	$[J]\theta^2$ UNPERTURBED	$[J]\theta^2$ EXPER.		$[J]\theta^2$ WITH R.P.C.
$K=\frac{1}{2}$ (#9)	0	$\frac{1}{2}+$	2.0	2.0		2.0
	.982	$\frac{3}{2}+$	1.8	1.8	4.9	3.5
	1.692	$\frac{5}{2}+$	1.0	1.1		0.9
$K=\frac{1}{2}$ (#11)	3.470	$\frac{1}{2}+$	1.7	1.8		0.9
	3.757	$\frac{3}{2}+$	3.0	2.4	4.2	1.6
	5.75	$\frac{5}{2}+$	.09	—		.007
$K=\frac{3}{2}$ (#8)	6.07	$\frac{3}{2}+$	4.6	1.1	—	1.8

EXPER. SUM

Fig. 7

tributions, ℓ_n values, and reduced widths have been obtained for many of the levels below 5 Mev excitation. As for other (1d,2s) shell nuclei being studied in this laboratory, the purpose is to examine in some detail the applicability of the collective model.

Preliminary data for the ℓ_n values and the reduced widths are generally in good agreement with published data.[11] Reduced widths not heretofore published have been obtained for a number of levels, including in particular the levels at 1.37 Mev, 1.63 Mev, and 2.58 Mev. The assignments for these levels are $\ell_n = 2$; predominantly $\ell_n = 2$ with an $\ell_n = 0$ admixture; and $\ell_n = 2$, respectively. The level at 2.27 Mev was previously reported [11] as being $\ell_n = 2$ with an $\ell_n = 0$ admixture which would fix the spin of this state as 2^+ or 3^+ since the ground state spin of Al^{27} is 5/2+. The angular distribution measured here does not clearly show any $\ell_n = 0$ component. It is interesting to note that the level at 1.37 Mev is the final state in the β decay from Mg^{28}. This transition is allowed and has a log ft = 4.4. Presumably this is a state involving double nucleon excitation, yet the level shows the characteristic stripping pattern. Further comments on this level appear in the following discussion.

In terms of the Nilsson diagram (Fig. 3), one might expect in the $Al^{27}(d,p)Al^{28}$ reaction the following particle configurations to show characteristic stripping distributions:

Al^{27} + neutron in orbit #9 giving rise to rotational bands with K = 2 and K = 3.

Al^{27} + neutron in orbit #11 giving rise to rotational bands with K = 2 and K = 3.

Al^{27} + neutron in orbit #8 giving rise to rotational bands with K = 1 and K = 4.

The negative parity bands are not considered here.

Low-lying levels which would not be expected to show a characteristic stripping angular distribution can arise from a particle configuration with two nucleons in orbit #9. There is evidence form the β decay that this configuration is responsible for the level at 1.37 Mev. On the basis of the rotational model, this configuration should not interact with the three configurations listed above through the RPC, but could mix through a direct interaction between the odd nucleons. Possibly this explains the well-defined stripping angular distribution for the 1.37-Mev level.

Figure 8 shows some of the stronger low-lying levels in the Al^{28} spectrum which one might hope to account for on the basis of a nuclear model.

---

11. MIT Progr. Rept. XV (1955-56); quoted in M. H. Macfarlane and J. B. French, Rev. Mod. Phys., 32, 582 (1960).

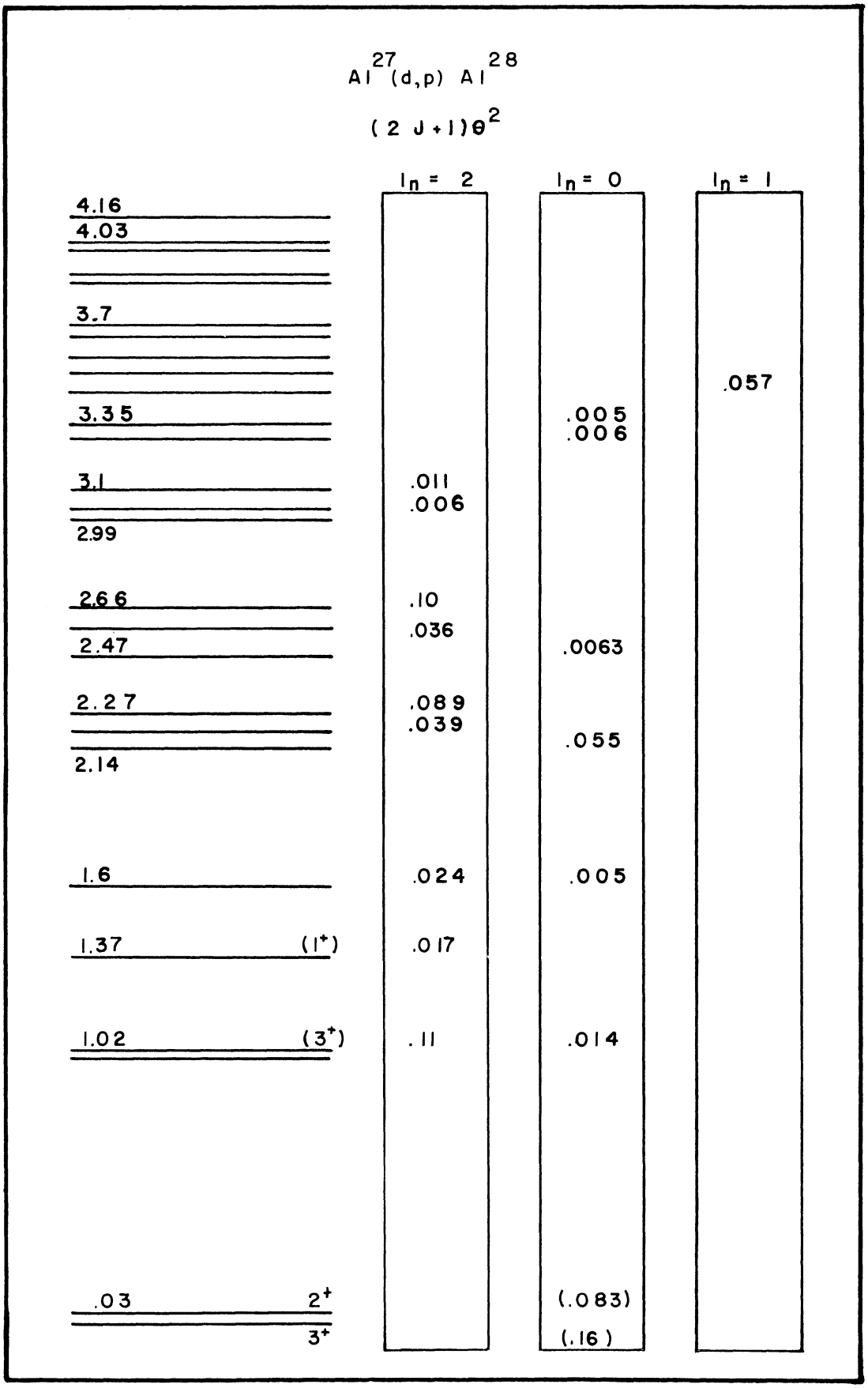
$Al^{27}(d,p)\ Al^{28}$
$(2J+1)\theta^2$
$l_n = 2$
$l_n = 0$
$l_n = 1$
4.16
4.03
3.7
3.35
3.1
2.99
2.66
2.47
2.27
2.14
1.6
1.37 (1^+)
1.02 (3^+)
.03 2^+
3^+
.011
.006
.10
.036
.089
.039
.024
.017
.11
.005
.006
.0063
.055
.005
.014
(.083)
(.16)
.057

Fig. 8

If one ignores the weak levels and asks if the rotational model can account for the strong $\ell_n = 0$ and $\ell_n = 2$ levels, in particular the four rather strong $\ell_n = 2$ levels between 2 and 2.7 Mev, the answer seems to be qualitatively "yes," provided it is assumed that the low-lying levels of bands formed when the neutron is put into orbits #11 and #8 fall into the region between 2 and 2.7 Mev and provided RPC is ignored. However, the six bands mentioned previously are coupled (directly or indirectly) through the RPC.

Attempts have been made to predict quantitatively the effects of the RPC on the energies and reduced widths. Matrix elements of the rotational Hamiltonian with the RPC connecting the six bands are shown in Fig. 9. The RPC connects states if they have the same spin I, $\Delta K = \pm 1$, and if for one nucleon, $\Delta\Omega = \pm 1$. In the figure, B is the rotational constant; $\hbar^2/2\mathcal{I}$. The E's, which have been chosen empirically, include the individual particle energies, effects of pairing and direct interactions, and all spin-independent terms in the rotational Hamiltonian.

The off-diagonal terms give the effects of RPC. The decoupling parameter "a" connects the two bands of the same particle configuration; the term "A" connects rotational bands of different particle configurations. The matrix is Hermitian; terms below the diagonal have been omitted. The matrix is the fully developed 6 x 6 matrix only if $I \geq 4$. For example, if I = 2, it collapses to a 3 x 3 matrix.

The matrices have been diagonalized using an IBM 704 computer for several values of the deformation parameter β, the rotational constant B, and the six empirical constants E in an attempt to fit the strong $\ell_n = 0$ and $\ell_n = 2$ levels. The results indicate:

1. Probably $\beta \leq .15$.

2. The calculated reduced widths for the ground state and the 1st and 3rd excited states compare favorably with the experimental results.

3. It does not seem possible, using only the configurations which lead to the six bands discussed, to fit four relatively strong $\ell_n = 2$ levels in the region between 2 and 2.7 Mev. Three of these levels would be assigned spin values I = 4.

With such close-lying levels, as mentioned in 3, RPC effects are very large. For example, they would always push one of the $\ell_n = 2$ levels below 2 Mev and thus near the 1.63-Mev level which has a definite $\ell_n = 0$ component and the other level into the region around 3 Mev where no strong $\ell_n = 2$ transition is observed. On the other hand, if it is assumed that the low-lying levels of the K = 1 and K = 4 bands lie considerably above the lowest levels of the second K = 2 and K = 3 bands, then two relatively strong $\ell_n = 2$ transitions between 2 and 2.7 Mev cannot be accounted for. As an alternative explanation, a configuration obtained by lifting a proton from the $\Omega = 3/2$ orbit (#7) to the

	n Orbit 9 $\Omega_p=\frac{5}{2},\Omega_n=\frac{1}{2}$		n Orbit 11 $\Omega_p=\frac{5}{2},\Omega_n=\frac{1}{2}$		n Orbit 8 $\Omega_p=\frac{5}{2},\Omega_n=\frac{3}{2}$	
	K=2	K=3	K=2	K=3	K=1	K=4
K=2	$E_2+BI(I+1)$	$-a_9B\sqrt{I(I+1)-6}$	0	$-BA_{9\,11}\sqrt{I(I+1)-6}$	$-BA_{8\,9}\sqrt{I(I+1)-2}$	0
K=3		$E_3+BI(I+1)$	$-BA_{9\,11}\sqrt{I(I+1)-6}$	0	0	$-BA_{8\,9}\sqrt{I(I+1)-12}$
K=2			$E_2'+BI(I+1)$	$-a_{11}B\sqrt{I(I+1)-6}$	$-BA_{8\,11}\sqrt{I(I+1)-2}$	0
K=3				$E_3'+BI(I+1)$	0	$-BA_{8\,11}\sqrt{I(I+1)-12}$
K=1					$E_1''+BI(I+1)$	0
K=4						$E_4''+BI(I+1)$

Fig. 9

$\Omega = 5/2$ orbit (#5) could interact strongly through RPC with the ground-state configuration. This multiply-excited state might then have a relatively strong admixture of the single-neutron excitation and thus give rise to a characteristic stripping angular distribution. With the limited experimental information now available, it is not feasible to investigate such a proposal quantitatively.

The general conclusions that can be drawn from this study to date are:

1. Although ℓ_n values and reduced widths are known for many of the levels in Al^{28}, the experimental data are still insufficient to permit a reasonably valid comparison of this nucleus with the collective model. In particular, additional information from sources other than the (d,p) reaction is needed for the levels between 2 and 3 Mev.

2. RPC plays a significant role in coupling the various K-bands.

3. Coupling between levels based on single-nucleon excitation and levels based on multiple-nucleon excitations must be considered.

D. THE LEVEL STRUCTURE OF P^{32}

The levels of P^{32}, an odd-odd nucleus in the (1d,2s) shell, have been studied by means of the (d,p) reaction up to an excitation of 5 Mev and angular distributions and reduced widths obtained for a number of them.[12] Targets of Li_3PO_4 and P_2O_5 evaporated on gold leaf were used.

The (d,p) spectrum for P^{32} has been measured by Piraino, Paris, and Buechner,[13] who list 52 levels up to an excitation of 6.2 Mev. Angular distributions for most of these levels up to 5 Mev excitation energy have been obtained here. Several of these angular distributions have also been measured previously.[14,15] A comparison shows, in general, good agreement with the present measurements.

Typical angular distributions are shown in Fig. 10. The 1.149-Mev and 2.223-Mev levels [Fig. 10 (a) and (b)] were previously interpreted[14] as $\ell_n = 0$. Because of the difference in the differential cross sections around 30° where the $\ell_n = 2$ curve is expected to peak, it is concluded that the 2.22-Mev level is a mixture of $\ell_n = 0$ and $\ell_n = 2$. Figure 10 (c) and (f) show distributions obtained that are interpreted as $\ell_n = 2$ and $\ell_n = 1$, respectively. Both distributions differ noticeably from the Butler curves at higher angles. The distributions obtained for two very weak levels are shown in Fig. 10 (d) and (e).

---

12. T. Holtebekk, Bul. Am. Phys. Soc. II 6, 259 (KA4) (1961).

13. Piraino, Paris, and Buechner, Phys. Rev. 119, 732 (1960).

14. Dalton, Hinds, and Parry, Proc. Phys. Soc. 70A, 586 (1957).

15. W. C. Parkinson, Phys. Rev. 110, 485 (1958).

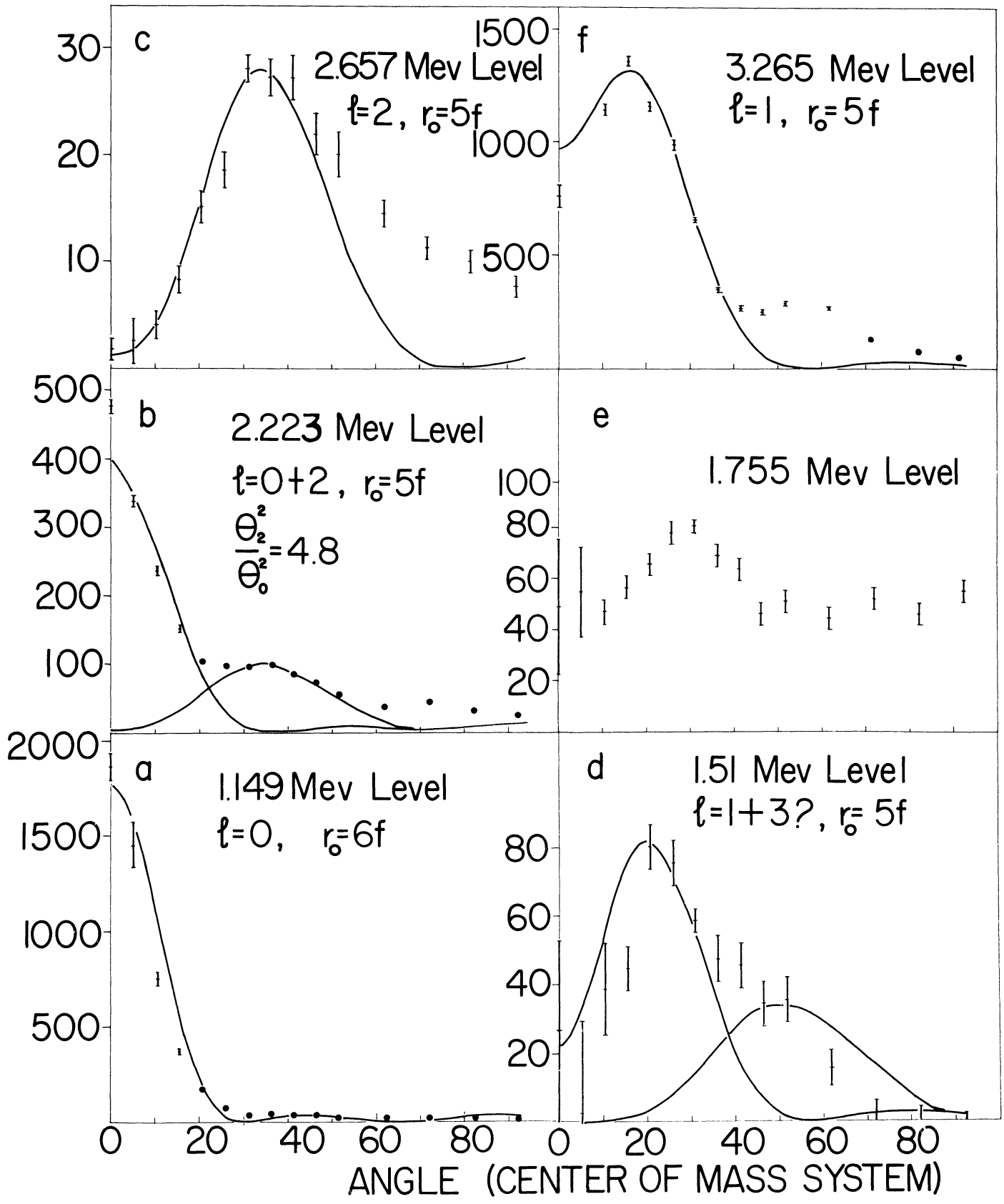
c
2.657 Mev Level
ℓ=2, r₀=5f
f
3.265 Mev Level
ℓ=1, r₀=5f
b
2.223 Mev Level
ℓ=0+2, r₀=5f
θ₂²/θ₀²=4.8
e
1.755 Mev Level
a
1.149 Mev Level
ℓ=0, r₀=6f
d
1.51 Mev Level
ℓ=1+3?, r₀=5f
ANGLE (CENTER OF MASS SYSTEM)

Fig. 10

The 1.51-Mev level, not previously reported, has a very low intensity at angles above 70°, no assignment of ℓ_n-values has been made to these levels.

Table II lists the information obtained for the levels up to 5-Mev excitation in P^{32}. With the exception of the 1.51-Mev level, the energies given are these reported by Piraino et al.[13]

Three levels near 4 Mev (3.994, 4.010, and 4.040), separated by 15 and 30 kev, respectively, have not yet been completely resolved. One of these, at 4.040 Mev, shows a strong $\ell_n = 1$ transition and one of the others seems to be a weak $\ell_n = 0$ level comparable in strength with the 4.21-Mev level. The levels at 3.80 Mev and 3.89 Mev are masked by an oxygen peak at angles in the region of 20°-30°. The shape of the angular distributions, however, indicates that they are not characteristic strong stripping levels. Those levels for which no ℓ_n values are listed are weak and show no typical stripping pattern.

At low excitation there are two levels which are mainly $\ell_n = 0$ and a third level with a strong $\ell_n = 0$ component. The relative strengths are roughly in the ratio 2:4:1. The ground state is known[15] to be mainly $\ell_n = 2$ with about 5% $\ell_n = 0$ mixture. In this region there are three strong $\ell_n = 2$ levels, two of medium strength and two, or possibly more, weak levels (reduced width less than 0.10 of the ground state). There are five odd-parity levels ($\ell_n = 1$) below 5-Mev excitation energy.

An attempt has been made to compare these experimental results with predictions of the collective model using Nilsson wave functions. The P^{31} nucleus has been discussed in terms of the Nilsson model by Broude, Green, and Willmott.[16] They assume a small negative deformation and a ground-state configuration with two neutrons and one proton in orbit #9. The extra neutron in P^{32} should then be captured in either orbit #8 or #11. There are, however, several other possible configurations, for example, configurations where either two neutrons and/or the proton are in orbit #8 or #11. The energy difference between this configuration and the ground-state should be small. These configurations based on multiple nucleon excitation will be reached through compound nucleus formation, but at least some, because of rotational-particle coupling with the ground-state configuration, should also be excited by the (d,p) stripping reaction. If, however, the coupling is not strong, which will be the case if the nuclear deformation is small, the intense levels should all arise from configurations where the neutron pair and the proton are in orbit #9.

The level scheme as predicted from the Nilsson diagram when rotation-particle coupling is neglected is shown in Fig. 11. The neutron can be captured in orbit #8 ($\Omega = 3/2$), resulting in rotational bands with K = 2 or 1; rotational bands with K = 1 or 0 arise when the neutron is captured in orbit #11 ($\Omega = 1/2$). The bands based on the $\Omega_n = 3/2$ levels should be reached by $\ell_n = 2$ reactions

16. Broude, Green, and Willmott, Proc. Phys. Soc. 72A, 1115 (1958).

TABLE II

LEVELS IN P^{32} FROM THE REACTION $P^{31}(d,p)P^{32}$

Q_o = 5.709 Mev; E_d = 7.77 Mev

Excitation Energy*	ℓ_n	$(2J+1)\theta^2$
0	0 + 2	0.15(ℓ=0), 3(ℓ=2)
0.077	2	4.4
0.516	0	0.65
1.149	0	1.2
1.322	-	-
1.51 ± .02	-	-
1.755	-	-
2.177	-	-
2.223	0 + 2	0.32(ℓ=0), 1.1(ℓ=2)
2.657	2	0.30
2.743	2	0.10
3.007	2	0.33
3.148	2	0.15
3.265	1	4.6
3.324	2	2.0
3.447	2	3.7
3.798	-	-
3.890	-	-
3.994	-	-
4.010	-	-
4.040	1	3.3
4.158	-	-
4.209	0	0.50
4.280	-	-
4.316	-	-
4.412	1	0.21
4.560	-	-
4.615	-	-
4.664	1	1.6
4.878	1	2.0

*Energies given by reference (13 except for the 1.51-Mev level.

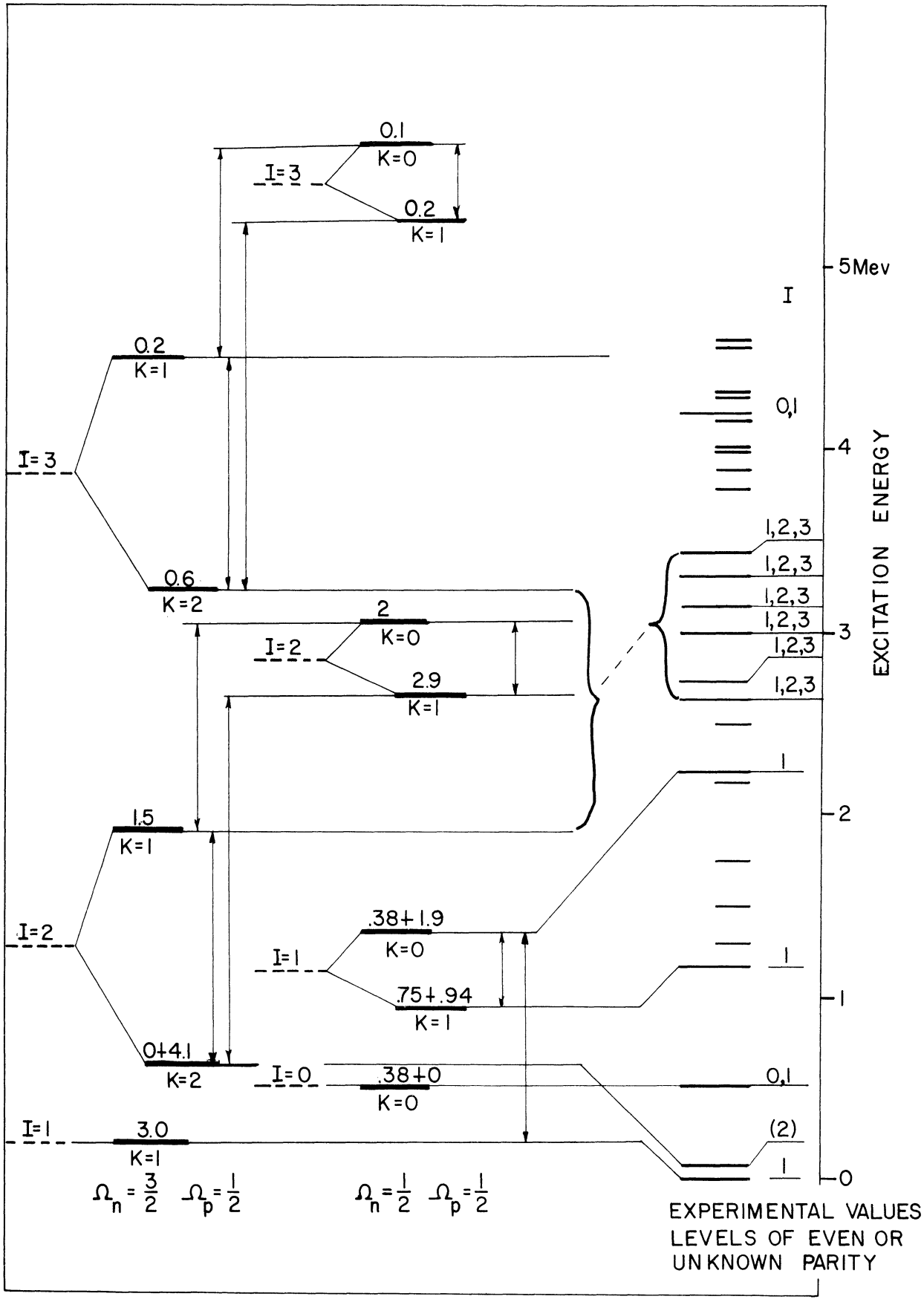
0.1
K=0
I=3
0.2
K=1
5Mev
I
0.2
K=1
0,1
I=3
4
1,2,3
1,2,3
1,2,3
1,2,3
1,2,3
1,2,3
0.6
K=2
2
K=0
I=2
2.9
K=1
3
EXCITATION ENERGY
1
1.5
K=1
2
.38+1.9
K=0
I=2
I=1
1
.75+.94
K=1
1
0+4.1
K=2
I=0
.38+0
K=0
0,1
I=1
3.0
K=1
(2)
1
0
$\Omega_n = \frac{3}{2}$ $\Omega_p = \frac{1}{2}$
$\Omega_n = \frac{1}{2}$ $\Omega_p = \frac{1}{2}$
EXPERIMENTAL VALUES
LEVELS OF EVEN OR
UNKNOWN PARITY

Fig. 11

only, whereas the $\Omega_n = 1/2$ bands may be reached through mixtures of $\ell_n = 2$ and $\ell_n = 0$. Levels which will interact through rotation-particle coupling are also indicated in Fig. 11.

In comparing the experimental data with the gross predictions of the model, the following facts emerge. One I = 0 level is expected and there is only one candidate for this in the low-energy region, the level at 0.516 Mev. The two I = 1 levels which should be reached through $\ell_n = 0$ and $\ell_n = 2$ admixture are identified with the 1.15-Mev and 2.22-Mev levels. The relative strength of the $\ell_n = 0$ components assuming no rotation-particle coupling should be 2:4:2 whereas the observed ration is 2:4:1. Any $\ell_n = 2$ admixture (predicted to be 50%) in the 1.15-Mev level is too small to be detected from the measurements; while the observed admixture (75%) for the 2.22 Mev level is that expected. These ratios are very sensitive to the deformation and the good agreement is probably coincidental. The ground state, with 5% $\ell_n = 0$ admixture in the predominantly $\ell_n = 2$ transition, is assumed to be the lowest level of the $\Omega_n = 3/2$ band. The $\ell_n = 0$ contribution must arise from interactions with other levels, probably the I = 1, K = 0 level. There is no information for identifying the rest of the $\ell_n = 2$ levels. Five rather strong $\ell_n = 2$ levels are expected in this region; there are 3 strong, 2 of intermediate strength, and 2 or more weak. The weak-stripping levels and other weak levels can presumably be accounted for by multiple excitation.

While there seems to be good agreement between the number of levels found and the number expected on the basis of the collective model, it is not yet possible to obtain quantitative agreement for either the energies or the reduced widths.

E. THE LEVEL STRUCTURE OF S^{33} AND S^{35}

The levels of S^{33} and S^{35}, both even-odd nuclei, have been studied[17] by means of the (d,p) reaction up to an excitation of 6 Mev and 2.5 Mev, respectively, and angular distributions and reduced widths obtained for most of them.

The spectrum of S^{33} is well known from the work of Endt and Paris[18] and contains more than 100 levels up to an excitation energy of about 7.5 Mev. In S^{35} only a few strong levels have been reported.[18] Additional information on S^{33} is available from the level scheme of the corresponding mirror nucleus Cl^{33}, from the branching in the β-decay of Cl^{33}, from neutron-capture γ rays, and from (d,p) angular distributions measured by Holt and Marsham[19] and by Middleton

17. J. Janecke, Bul. Am. Phys. Soc. II 6, 259 (KA5) (1961).

18. P. M. Endt and C. H. Paris, Phys, Rev. 110, 89 (1958).

19. T. R. Holt and T. N. Marsham, Proc. Phys. Soc. A 66, 467 (1953).

and Hinds.[20] These known data are essentially in agreement with the present experimental results.

Figure 12 shows the proton spectra obtained from the deuteron bombardment of CdS, both with natural sulphur and sulphur enriched in S^{34}. The excitation energies listed are those of Endt and Paris.[18] Most of the known S^{33} lines could be resolved. In the spectrum taken with the enriched target many of the levels of S^{33} are still evident, but there are in addition many levels indicated with arrows which are not yet identified. Further work remains before the levels can be definitely assigned to states of S^{35}.

In the measured angular distributions of the S^{33} levels up to an excitation energy of 6.1 Mev, probably no $\ell_n = 0$ and $\ell_n = 1$ levels and no strong $\ell_n = 2$ and $\ell_n = 3$ levels have been missed. In addition, the angular distributions of three S^{35} levels have been measured. Reduced widths have been obtained for those levels which show characteristic stripping patterns.

Figures 13 and 14 show the angular distributions from the ground state up to the seventh excited state in S^{33}. The Butler curves are all calculated with a radius of 5.6 f except for the $\ell_n = 0$ first-excited state at 0.839 Mev where a radius of 6.6 f was used. The significant features of these results are: The third-excited state which is interpreted as $\ell_n = 2$ has not been previously reported. The second-excited state at about 2 Mev shows no clear stripping and no clear isotropic distribution. The three levels near 3 Mev excitation have not been resolved previously in angular-distribution measurements. The $\ell_n = 2$ level near 3 Mev is the final state for the 0.3% component of the Cl^{33} β-decay.

The level schemes of S^{33} and S^{35} together with the measured ℓ_n values and the reduced widths are shown to the right in Fig. 15. The levels of S^{33} are split into three groups, those with even ℓ_n, those with odd ℓ_n, and those that are isotropic or weak. The known S^{35} level scheme is shifted such that the strong $\ell_n = 3$ level matches the strong $\ell_n = 3$ level in S^{33}.

An attempt has been made to compare the measured level structure of S^{33} with the predictions of the collective model using the Nilsson diagram. S^{32}, with 16 protons and 16 neutrons, fill all orbits up to and including the $2s_{1/2}$ shell. The captured neutron in S^{33} should therefore enter the $d_{3/2}$ shell, in either the orbit with $\Omega = 1/2$ or the orbit with $\Omega = 3/2$. The quadrupole moment of S^{33} is reported as being negative which probably indicates negative deformation. The neighboring even-odd nucleus P^{31} is also known[16] to have negative deformation. The deformation cannot be derived from the known magnetic moment because the ground state is a mixture of $\Omega = 1/2$ and $\Omega = 3/2$, hence the magnetic moment depends not only on δ, but also on the mixing ratios.

The level sequence shown on the left of Fig. 15 was obtained assuming

20. R. Middleton, private communication.

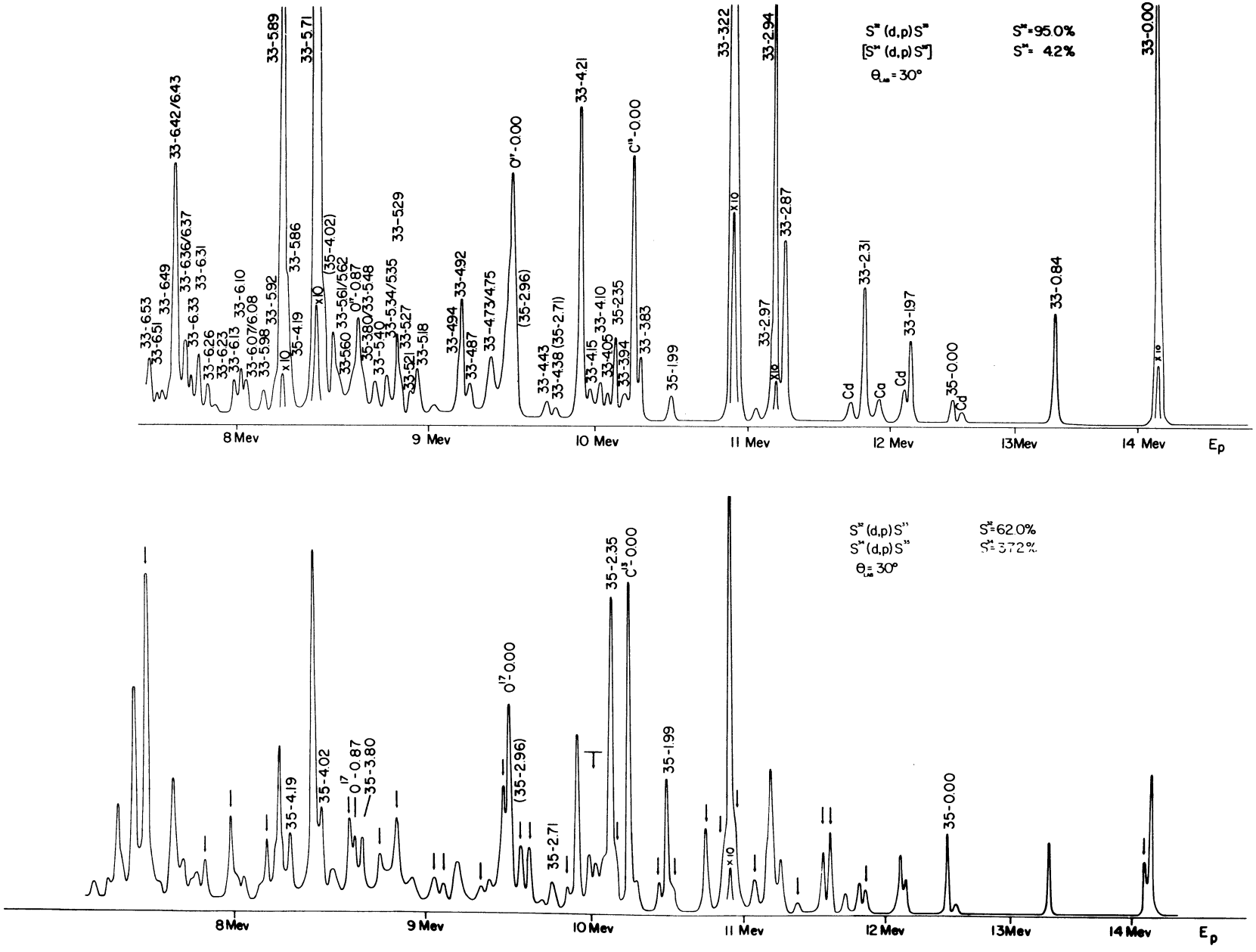
S³³ (d,p) S³³
[S³⁴ (d,p) S³⁵]
θ_lab = 30°
S³³=95.0%
S³⁴= 4.2%
33-000
33-322
33-294
33-589
33-571
33-421
C¹³-0.00
0¹⁷-0.00
33-287
33-231
33-197
33-084
35-235
35-199
35-000
33-642/643
33-649
33-636/637
33-631
33-626
33-623
33-613
33-610
33-607/608
33-598
33-592
33-586
35-419
35-402
33-561/562
0¹⁷-0.87
35-380/33-548
33-540
33-534/535
33-529
33-527
33-521
33-518
33-494
33-492
33-487
33-473/475
0¹⁷-0.00
(35-2.96)
33-443
33-438 (35-2.71)
33-415
33-410
33-405
33-394
33-383
33-2.97
Cd
Ca
Cd
Cd
8 Mev
9 Mev
10 Mev
11 Mev
12 Mev
13Mev
14 Mev
Ep
S³⁴ (d,p) S³⁵
S³⁴ (d,p) S³⁵
θ_lab = 30°
S³⁴=62.0%
S³⁴= 37.2%
35-235
C¹³-0.00
0¹⁷-0.00
(35-2.96)
35-271
35-199
35-000
35-419
35-402
0¹⁷-0.87
35-380
8 Mev
9 Mev
10 Mev
11 Mev
12 Mev
13Mev
14 Mev
Ep

Fig. 12

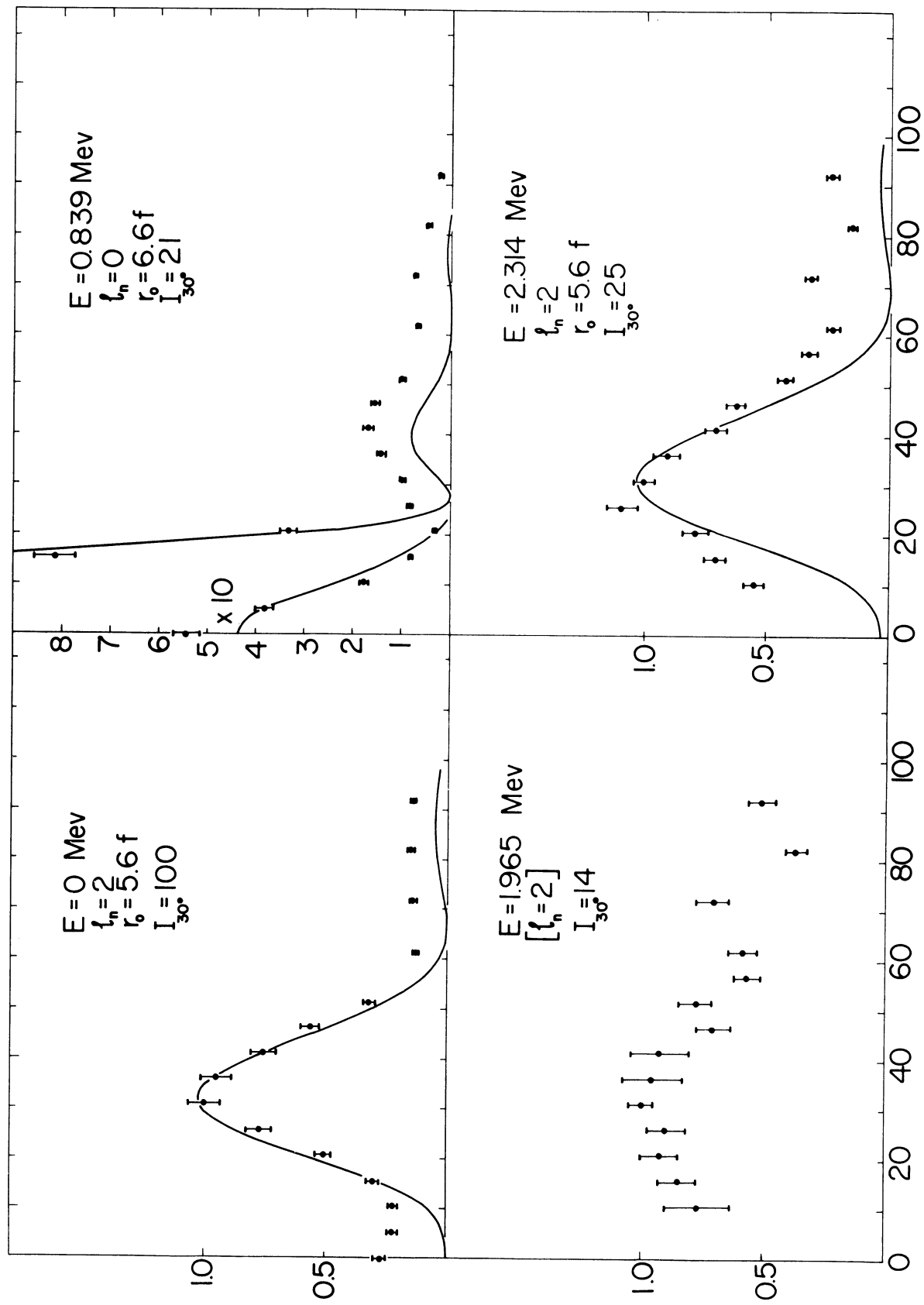
E = 0 Mev
$\ell_n = 2$
$r_o = 5.6$ f
$I_{30°} = 100$
E = 0.839 Mev
$\ell_n = 0$
$r_o = 6.6$ f
$I_{30°} = 21$
x 10
E = 1.965 Mev
$[\ell_n = 2]$
$I_{30°} = 14$
E = 2.314 Mev
$\ell_n = 2$
$r_o = 5.6$ f
$I_{30°} = 25$
θ_{cm}

Fig. 13

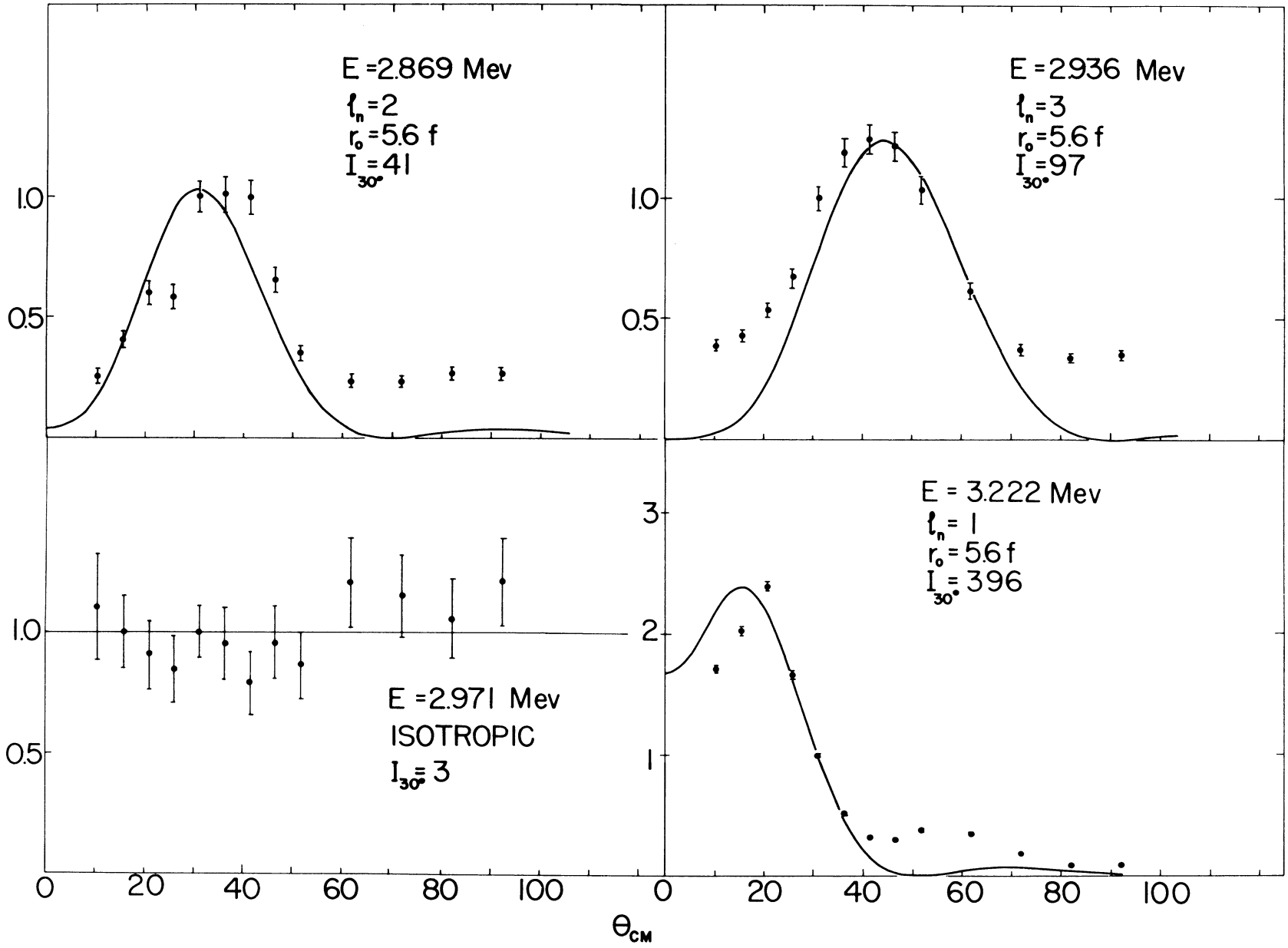
E =2.869 Mev
l_n=2
r_o=5.6 f
$I_{30°}$=41
E =2.936 Mev
l_n=3
r_o=5.6 f
$I_{30°}$=97
E =2.971 Mev
ISOTROPIC
$I_{30°}$= 3
E = 3.222 Mev
l_n= 1
r_o= 5.6 f
$I_{30°}$= 396
1.0
0.5
3
2
1
0
20
40
60
80
100
θ_{CM}

Fig. 14

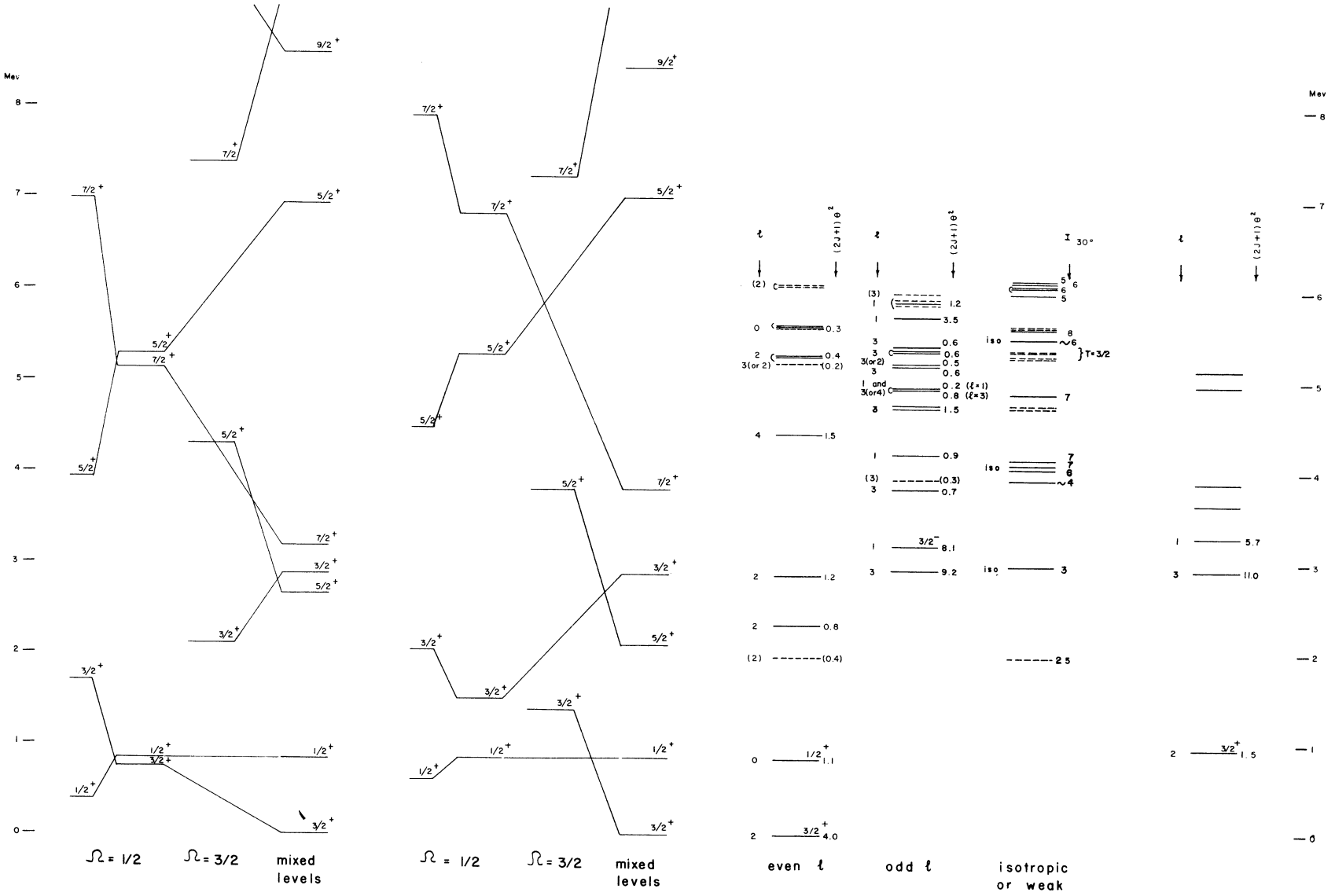
Mev
Ω = 1/2
Ω = 3/2
mixed levels
δ≈β = − 0.2
a = − 1.05 ħ²/2J
A = − 1.7 ħ²/2J
ħ²/2J = 0.44 Mev
Ω = 1/2
Ω = 3/2
mixed levels
δ≈β = − 0.3
a = − 0.55 ħ²/2J
A = − 1.7 ħ²/2J
ħ²/2J = 0.49 Mev
even ℓ
odd ℓ
isotropic or weak
S33 experimental
S35 exp

Fig. 15

deformations of $\beta = -0.2$ and -0.3. With these vaules of β, the decoupling parameter a and the rotation-particle coupling parameter A were calculated. From the position of the experimentally known $1/2^+$ level between the two $3/2^+$ levels, it follows that the $\Omega = 1/2$ band lies lowest. While this is in disagreement with the expectation for negative deformation on the basis of the Nilsson diagram, it is not surprising since it is known from Mg^{25}, and other examples, that such inversions occur. Assuming the strong $\ell_n = 2$ level at 2.9 Mev is the other $3/2^+$ level, the rotational energy $\hbar^2/2\mathfrak{I}$ and the spacing between the two bands can be calculated. Rotation-particle coupling mixes the two bands and shifts the levels as indicated. The $\ell_n = 2$ level at 2.3 Mev is evidently the $5/2^+$ member of the $\Omega = 3/2$ band, but it is not evident which level corresponds to the $7/2^+$ member; the $\ell_n = 4$ level or one of the weak levels are all candidates.

The reduced widths and the magnetic moment including rotation-particle coupling calculated for $\beta = -0.1$, -0.2 and -0.3 are given in Table III. While the reduced width for the excited $3/2^+$ level is in poor agreement, the magnetic moment is consistent with a deformation between -0.2 and -0.3.

In the region near 5 Mev there are several positive-parity states which correspond to known positive-parity states in the mirror nucleus Cl^{33}. These arise from the $g_{9/2}$ shell and the fact that they occur near 5 Mev also indicates relatively large deformation.

The odd-parity levels arise from the $1f_{7/2}$, $2p_{3/2}$, and $1f_{5/2}$ shells. It is expected that the many rotational bands will interact strongly and therefore a quantitative interpretation will be difficult.

The situation in S^{35} is expected to be similar to that in S^{33} for the odd-parity states if both nuclei have about the same deformation. However, because of the two additional neutrons, only one rotational band with even parity will arise from the $d_{3/2}$ shell. Measurements in process will confirm whether the ground state of S^{35} arises from the $\Omega = 3/2$ band or from the $\Omega = 1/2$ band.

The available experimental data are not in disagreement with the collective model, but further data must be obtained and the calculations extended before a more definite statement can be made.

F. THE LEVEL STRUCTURE OF Cl^{36} AND Cl^{38}

The work on the level structure of Cl^{36} and Cl^{38} is in the preliminary stage and there are no significant results to report. Natural chlorine targets have been prepared by evaporating AgCl on gold leaf. The proton spectrum at 30° has been obtained up to 7.5 Mev excitation and confirms the great majority of levels in Cl^{36} previously reported.[21] Angular distributions have been ob-

21. Paris, Buechner, and Endt, Phys. Rev. 100, 1317 (1955).

TABLE III

E_{exc}, Mev	J^{π}	Ω	$(2J+1)\theta^2_{theor}$ with RPC			$(2J+1)\theta^2_{exp}$
			$\beta = -0.1$	$\beta = -0.2$	$\beta = -0.3$	
0.000	$3/2^+$	1/2 (3/2)	4.0	4.0	4.0	4.0
0.839	$1/2^+$	1/2	0.25	0.59	0.70	1.0
2.314	$(5/2^+)$	3/2 (1/2)	0.15	0.80	1.87	0.8
2.869	$(3/2^+)$	3/2 (1/2)	1.16	0.32	0.01	1.2
---	$(5/2^+)$	1/2 (3/2)	0.01	0.00	0.00	-
		μ	1.26	0.87	0.48	0.63
		$(\%)^2_{K=1/2}$	0.73	0.91	0.52	-
		$(\%)^2_{K=3/2}$	0.27	0.09	0.48	-

tained for the levels up to an excitation energy of 4.5 Mev in Cl^{36}, but to date only the ground and first excited states have been analyzed. Both distributions correspond to a transition with $l_n = 2$, the experimental points being fitted quite well with Butler curves using radii of 5.8 f.

The identification of unknown levels observed in the AgCl spectrum and the measurement of l_n and the reduced widths is in progress.

G. DEUTERON ELASTIC SCATTERING

In the interpretation of stripping angular distributions it has been customary to use the Butler theory to determine the value of the orbital angular momentum of the captured nucleon and to extract the reduced widths. In many cases the interpretation of the angular distributions is difficult or ambiguous and it is well known that the absolute reduced widths have little meaning. This is not surprising in view of the approximations necessarily made in the theory at that time. More complete calculations have been made by several authors[22,23] by including Coulomb effects and by using distorted waves for the incoming deuteron and/or the outgoing proton. The parameters necessary for describing the distortion in the deuteron wave can be obtained from measurements of the elastic scattering of deuterons from the target nucleus involved.

The deuteron elastic scattering cross section for the isotopes currently being studied in this laboratory have been or are being measured.[24] To date relative cross sections have been obtained for Be^9, Na^{23}, Mg^{24}, Mg^{25}, Mg^{26}, Al^{27}, P^{31}, natural sulphur, nickel, and gold at a deuteron energy of 7.775 Mev, for laboratory angles from 30° to 95° using the magnetic analysis instrumentation associated with the 42-inch cyclotron. The current integrator and solid angle of the analyzer have been carefully calibrated and the relative cross sections are now being converted to absolute values.

Commercially available foils were used as targets for the measurements of Be, Al, Ni and Au, while thin films with gold leaf backing were used for Na^{23}, Mg^{24}, Mg^{25}, Mg^{26}, and Pl^{31}. Typical angular distributions are shown in Fig 16, where the ordinate is the ratio of the measured to the Coulomb cross section at the corresponding center-of-mass angle, plotted on a logarithmic scale. The same general pattern is evident for all the nuclei, minima occurring at about 45° and 90° and maxima at about 60° and possibly 30°. Measurements made using 4 Mev deuterons[25] show less deviation below Rutherford, while experiments

---

22. W. Tobocman and M. H. Kalos, Phys. Rev., 97, 132 (1955).

23. R. Huby, M. Y. Refai, and G. R. Satchler, Nuclear Phys. 9, 94 (1958).

24. Bardwick, Tickle, and Parkinson, Bul. Am. Phys. Soc. II 6, 259 (KA6) (1961).

25. I. Slaus and W. Parker Alford, Phys. Rev. 114, 1054 (1959).

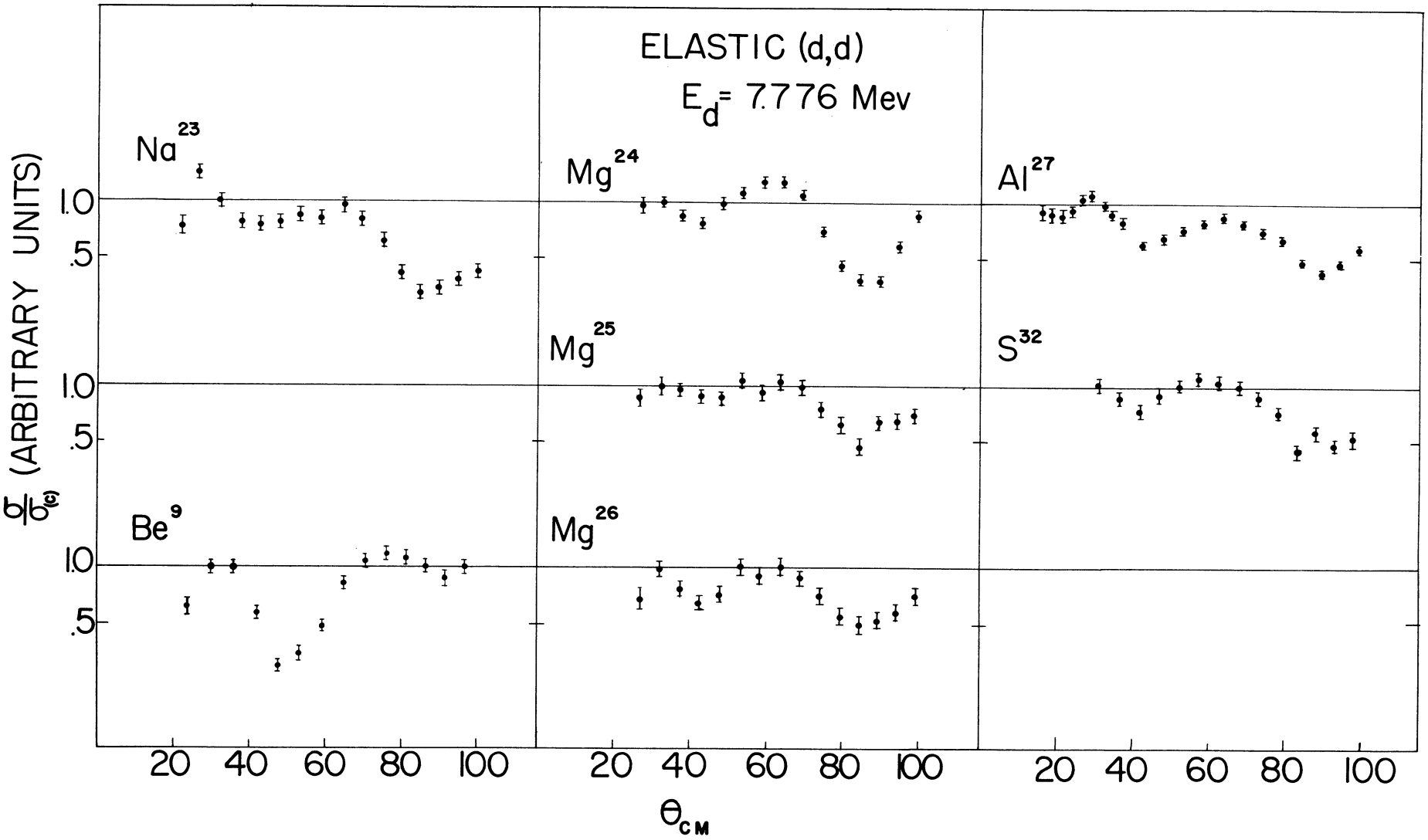
ELASTIC (d,d)
E_d = 7.776 Mev
Na^{23}
Mg^{24}
Al^{27}
Mg^{25}
S^{32}
Be^{9}
Mg^{26}
$\frac{\sigma}{\sigma_{(c)}}$ (ARBITRARY UNITS)
1.0
.5
20
40
60
80
100
θ_{CM}

Fig. 16

done at higher energies[26] show the deviation below Rutherford to begin at smaller angles. At higher energies, the peaks and valleys grow more pronounced and shift towards zero degrees.

Using the Oak Ridge code,* optical model parameters are being obtained from these data and when available they will be used as input information to calculate stripping angular distributions.

H. PROTON POLARIZATION IN THE $Be^9(d,p)Be^{10}$ REACTION

Polarization measurements of the proton groups corresponding to the ground and first-excited state of Be^{10}, reported in part last year, have been completed. The polarization has been measured at a deuteron energy of 7.8 Mev for proton laboratory scattering angles of 10°, 20°, 40°, 60°, and 80° for the ground-state reaction, and 20° and 40° for the first-excited state. In addition, to complete the information necessary for a distorted wave analysis, the differential cross section for the $Be^9(d,p)Be^{10}$ ground-state and the $Be^9(d,p)Be^9$ elastic scattering cross section have also been measured.[24]

The polarization measurements for the ground-state are as follows:

θ_{cm}	$P_p(\theta)$
11.4°	+0.24 ± 0.05
22.7°	+0.10 ± 0.03
45.0°	+0.16 ± 0.09
65.7°	+0.15 ± 0.06
86.5°	-0.42 ± 0.11

It should be noted that more careful measurements involving a background determination have slightly changed some of the values quoted last year. The axis of quantization for the measurements is given by the Basel convention. Two important conclusions can be drawn from the data:

(1) On the basis of the Distorted-Wave Born-Approximation Theory (DWBA), involving spin-independent distortion of the deuteron and the proton, the maximum predicted polarization is $P_{max} = 0.17$. This limit is clearly violated above and below the stripping peak ($\theta_{cm} \simeq 20°$), indicating the presence of spin-dependent forces.

*We are much indebted to Dr. G. R. Satchler for making available to us the code for doing these computations.

26. J. L. Yntema, Phys. Rev. 113, 261 (1959); J. R. Rees and M. B. Sampson, Phys. Rev. 108, 1289 (1957); Nishida, Progr. Theor. Phys. 19, 389 (1958); Cindro and Wall, Phys. Rev. 119, 1340 (1960).

(2) In the approximation that the deuteron and proton are only weakly distorted by the nuclear potentials, the radial cutoff form of the DWBA theory predicts that the polarization will change sign where the plane-wave cross section has its first minimum. A linear extrapolation between the 66° and 87° points indicates that the polarization sign change occurs at $\theta_{cm} = 71° \pm 4°$. On the other hand, the experimental differential cross section has its minimum at 53° while the first minimum in the Butler cross section ($\ell_n = 1$, $r = 5.2$ f) occurs at 60°. This result confirms the work of Hird and Strzalkowski[27] and indicates that contributions from the nuclear interior, and from the distortion of the deuteron and proton constitute an important part of the total stripping amplitude.

For kinematical reasons, measurements were restricted to 20° and 40° for the first-excited state of Be^{10}. Careful track-length analysis of the data has eliminated the sign discrepancy noted in last year's report and has produced the values $P = -0.14 \pm 0.04$ at $\theta_{cm} = 22.4°$ and $P = -0.49 \pm 0.09$ at $\theta_{cm} = 44.6°$. At 44.6° the polarization is in excess of the maximum predicted value of $P_{max} = -0.27$ for this state and again shows the presence of spin-dependent forces. Taylor[28] has previously measured the (d,pγ) angular correlation for the Be^{10} first-excited state at this laboratory. Analysis of Taylor's data[29] predicts that the DWBA parameter λ [23] has the value $\lambda = 1.1 \pm 0.4$ at $\theta_{cm} = 22°$, while analysis of the polarization data yields the value $\lambda = 0.86 \pm 0.12$. The agreement between the measurements is quite good. At 44.6°, λ is imaginary as a result of the large polarization so that no comparison is possible with (d,pγ) measurements on the basis of a spin-independent theory.

I. (d,n) REACTIONS BY TIME-OF-FLIGHT

The neutron time-of-flight spectrometer has been reactivated to study (d,n) reactions in the region of neutron energies from about 1 Mev up to the highest energies expected from reactions of interest. An over-all time resolution of 5 nanoseconds (5×10^{-9} sec) has been realized using flight paths of up to 9.6 meters, with provisions now being made to extend this length to 15 meters.

As described in previous reports, the normal cyclotron output consists of short deuteron bursts occurring once each oscillator period of about 100 nanoseconds, corresponding to a frequency of 10 mc/sec. The phase bunching inherent in the cyclotron provides an output pulse 4 nanoseconds in half-width. The original pulse system used to decrease the repetition rate to prevent excessive overlap of neutrons from one deuteron burst with those from the succeeding burst, has been replaced by an rf sweeper which permits one in four of the original beam pulses to reach the target. The d-c bias on the plates is arranged so

27. B. Hird and A. Strzalkowski, Proc. Phys. Soc. (London) A75, 868 (1960).

28. R. T. Taylor, Phys. Rev. 113, 1293 (1959).

29. F. H. Read, J. M. Calvert, and G. Schork, Nuc. Phys. 23, 386 (1961).

that only the beam pulse occurring at one peak of the applied rf is passed. A delay line variable from the control panel allows the sweeper voltage to be properly phased with respect to the main oscillator. A low-capacitance probe located directly behind the target is used to indicate proper beam pulsing.

Two detectors have been tried in this work. The first, a liquid scintillator (terphenyl in phenylcyclohexane), has been described in an earlier report. The second is a plastic scintillator of polystyrene mounted on a type 6342 photomultiplier. Both detectors are 5 inches in diameter and 3 inches thick. Results to date indicate that both detectors are essentially equivalent, although there is an indication that the liquid scintillator may have some advantages for gamma-ray versus neutron discrimination.

A block diagram of the apparatus is shown in Fig. 17. The timing system, which follows closely the Los Alamos design, is a time-to-pulse-height converter, the output of which is fed to a 256 channel pulse height analyzer. The "start" pulse is derived by amplification through distributed amplifiers of the detector photomultiplier anode pulse. These pulses cover a wide range in amplitude and to minimize the time jitter associated with the discriminator a parallel channel using conventional "slow" electronics is used to generate a gating pulse for the pulse height analyzer, but only after discrimination at a level corresponding to several volts above the fast discriminator. Thus only those start pulses which clear the fast discriminator by this amount give rise to a recorded event. While this does distort the recorded spectrum, relative intensities of neutron groups can be determined from calibration of the detector.

The "stop" pulse is generated by scaling down the 10-Mc cyclotron oscillator frequency by a factor of four (to 2.5 Mc) and shaping the signal to give a pulse with a fast rise time for every four cyclotron periods. Since the sweeper also operates at the same 2.5 Mc frequency, one stop pulse is generated per beam pulse at the target. The time separation between the stop and the beam pulses can be adjusted with a variable delay line in the stop chain.

The output of the converter does not give directly the neutron flight time, but rather the difference between the flight time and the time between stop pulses. Since the time between adjacent stop pulses is exactly equal to four cyclotron periods, it is accurately known, hence no uncertainty is introduced by using this indirect timing scheme. The scheme does have the great advantage that the converter action is started only by a detected event, and not by the much higher repetition rate of the beam pulses on the target. A long flight time thus corresponds to a small time interval between start and stop pulses. The zero time reference may be shifted along the display by varying the delay in the stop chain.

Since the detector is sensitive to gamma radiation as well as neutrons, each deuteron burst on the target gives rise to a prompt gamma-ray peak on the display at a time easily determined from the geometry. The gamma peak is then

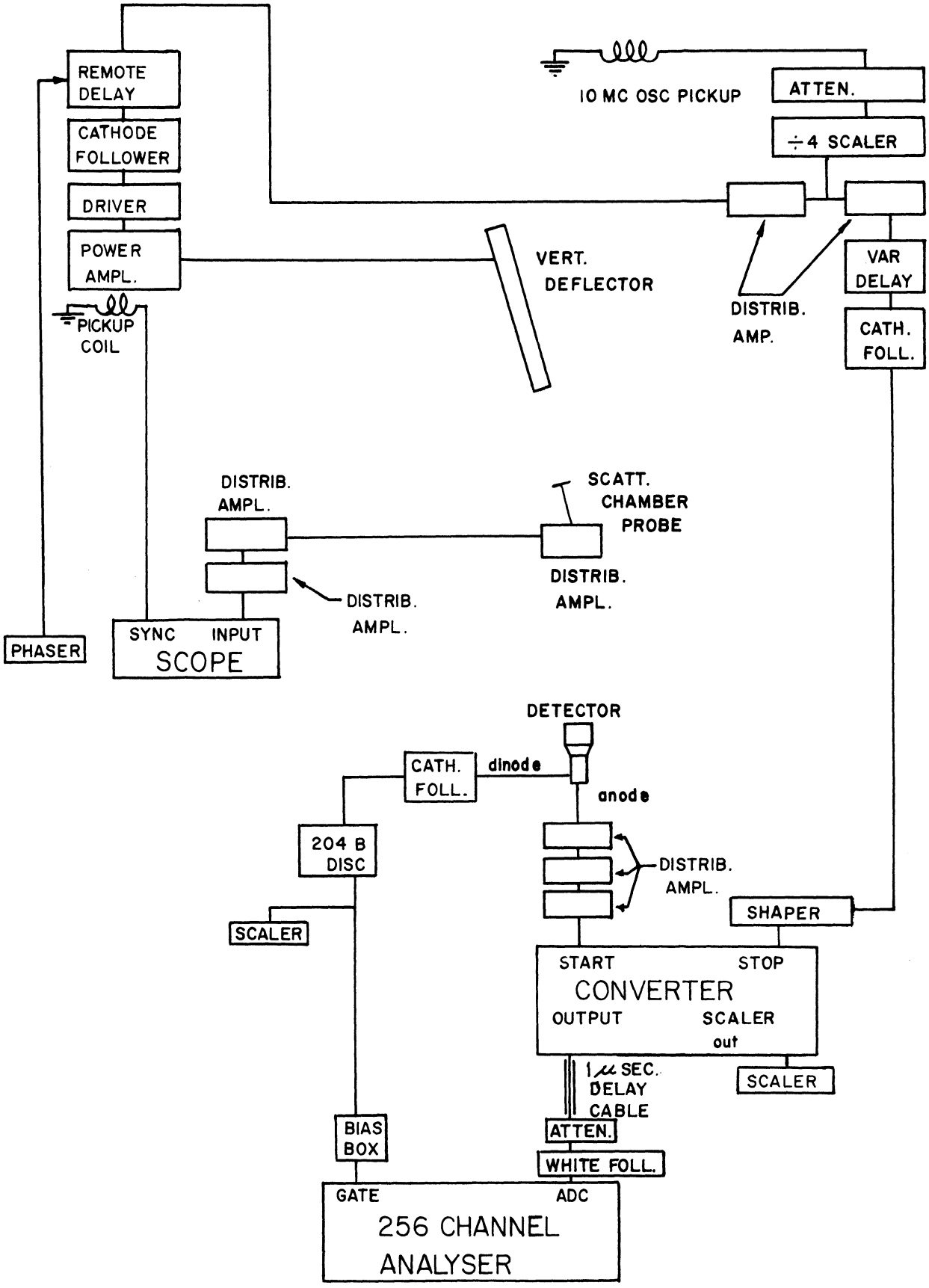
REMOTE DELAY
CATHODE FOLLOWER
DRIVER
POWER AMPL.
PICKUP COIL
PHASER
SYNC INPUT
SCOPE
10 MC OSC PICKUP
ATTEN.
÷4 SCALER
VERT. DEFLECTOR
DISTRIB. AMP.
VAR DELAY
CATH. FOLL.
DISTRIB. AMPL.
DISTRIB. AMPL.
SCATT. CHAMBER PROBE
DISTRIB. AMPL.
DETECTOR
CATH. FOLL.
dinode
anode
204 B DISC
SCALER
DISTRIB. AMPL.
SHAPER
START
STOP
CONVERTER
OUTPUT
SCALER out
SCALER
1 μ SEC. DELAY CABLE
ATTEN.
BIAS BOX
WHITE FOLL.
GATE
ADC
256 CHANNEL ANALYSER

Fig. 17

followed in time by the various neutron groups produced in the target. The spacing on the display between a given nuetron group and the gamma peak is then converted to neutron flight time and to energy. Typical flight times over the path lengths being used are from 200 to 800 nsec for neutrons of energies 15 Mev to 1 Mev. Because the sweeper period is 400 nsec, there is some overlap of the lower-energy neutrons from one burst with high-energy neutrons from the succeeding burst. Any ambiguity so introduced may be resolved, however, by noting the shift along the display of each observed peak with changes in path length. The obvious disadvantages of the possible ambiguity is, however, more than offset by the improvement gained in timeing accuracy. This follows from the fact that another gamma peak will be located in general much closer to a neutron group of interest than to the original gamma peak. By proper choice of path length this spacing can be reduced to zero, in which case the neutron flight time is known to the same precision as the period of the sweeper with no assumptions necessary regarding the converter linearity.

The measurements to date have been directed toward studying the properties of the system as a neutron spectrometer. A spectrum taken with a mylar target containing both carbon and oxygen is shown in Fig. 18. Three neutron groups are observed corresponding to the energies expected from the ground, first-excited, and second-third (unresolved) excited levels in N^{13} and two groups are observed which correspond to the ground and first-excited levels in F^{17}. To date the best time spread (full width at half maximum) obtained for the gamma-ray peak is 5 nsec, of which 4 nsec results from the finite width of the deuteron burst on the target.

Future work will concentrate on reducing the low pulse height background which makes observation of low-energy neutrons difficult. This will allow a more complete coverage of the spectra from many nuclei of interest.

J. SOLID-STATE PARTICLE DETECTORS

The development of the solid-state ionization devices described in the last report has been completed and they now form a useful adjunct to the total instrumentation available for nuclear spectroscopy. The "parallel-plate" ionization chamber made from n-type silicon counter-doped with gold has proved to be more useful than the gold-germanium surface barrier detector. Detectors in the form of an array as shown in Fig. 10 of the 1960 report are being used at the image plane of the magnetic analysis system while single crystals of various sizes are being used for low resolution studies. The characteristics and principles of operation are described[30] in a forthcoming publication and thus need not be presented here. An example of the kind of results obtained with the 20- channel array is given in Fig. 19 where the data are compared with those obtained using nuclear emulsions for protons groups from the ground state of

30. W. C. Parkinson and O. M. Bilaniuk, Rev. Sci. Insts. (in press).

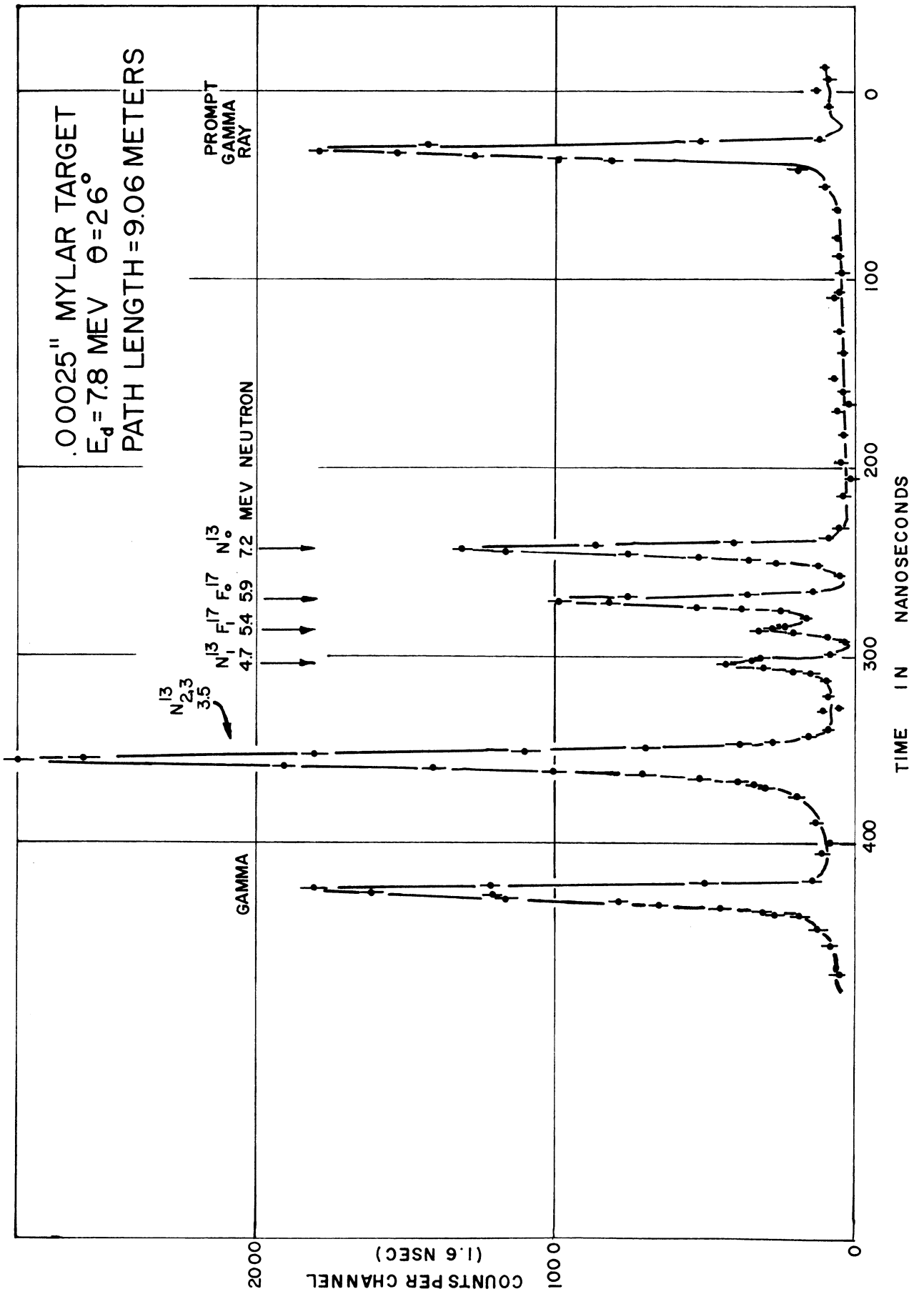
.00025" MYLAR TARGET
E_d = 7.8 MEV θ=26°
PATH LENGTH=9.06 METERS
PROMPT GAMMA RAY
N^{13} 7.2 MEV NEUTRON
F^{17}_0 5.9
F^{17}_1 5.4
N^{13}_1 4.7
$N^{13}_{2,3}$ 3.5
GAMMA
COUNTS PER CHANNEL (1.6 NSEC)
2000
1000
0
0
100
200
300
400
TIME IN NANOSECONDS

Fig. 18

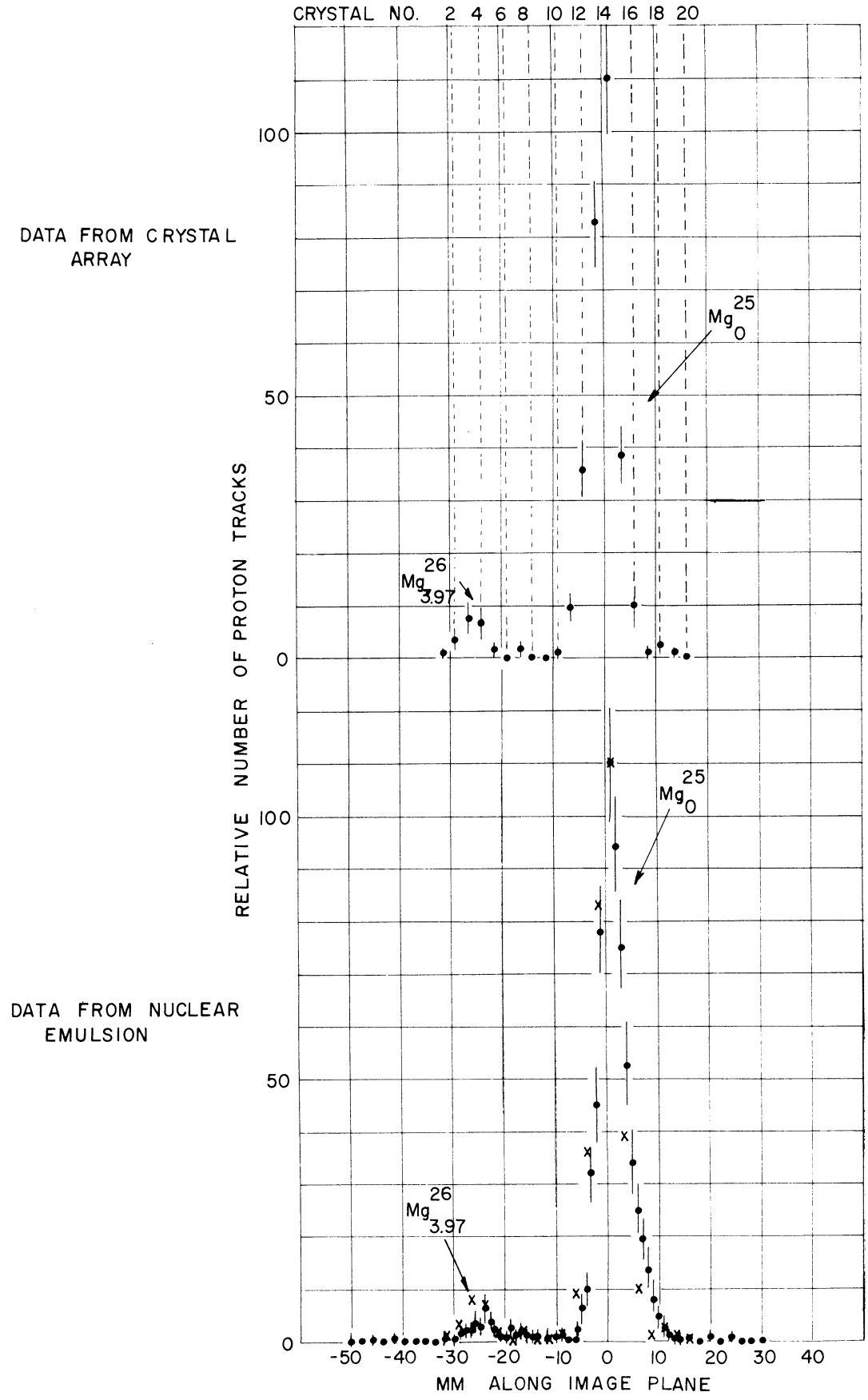
CRYSTAL NO. 2 4 6 8 10 12 14 16 18 20
DATA FROM CRYSTAL ARRAY
DATA FROM NUCLEAR EMULSION
RELATIVE NUMBER OF PROTON TRACKS
100
50
0
100
50
0
Mg^{25}_{0}
$Mg^{26}_{3.97}$
Mg^{25}_{0}
$Mg^{26}_{3.97}$
-50 -40 -30 -20 -10 0 10 20 30 40
MM ALONG IMAGE PLANE

Fig. 19

Mg^{25} and from the 3.97-Mev level in Mg^{26} in the Mg(d,p) reaction. The crosses on the lower curve are the data points form the crystal array. An example of a "poor-resolution" spectrum taken with a single crystal is shown in Fig. 20 for the reaction Al^{27}(d,p)Al^{28}. The resolution has been intentionally reduced to 400 kev by using a thick target and absorber foils in front of the crystal. The purpose here is to display the "gross-structure" properties of Al^{28}.

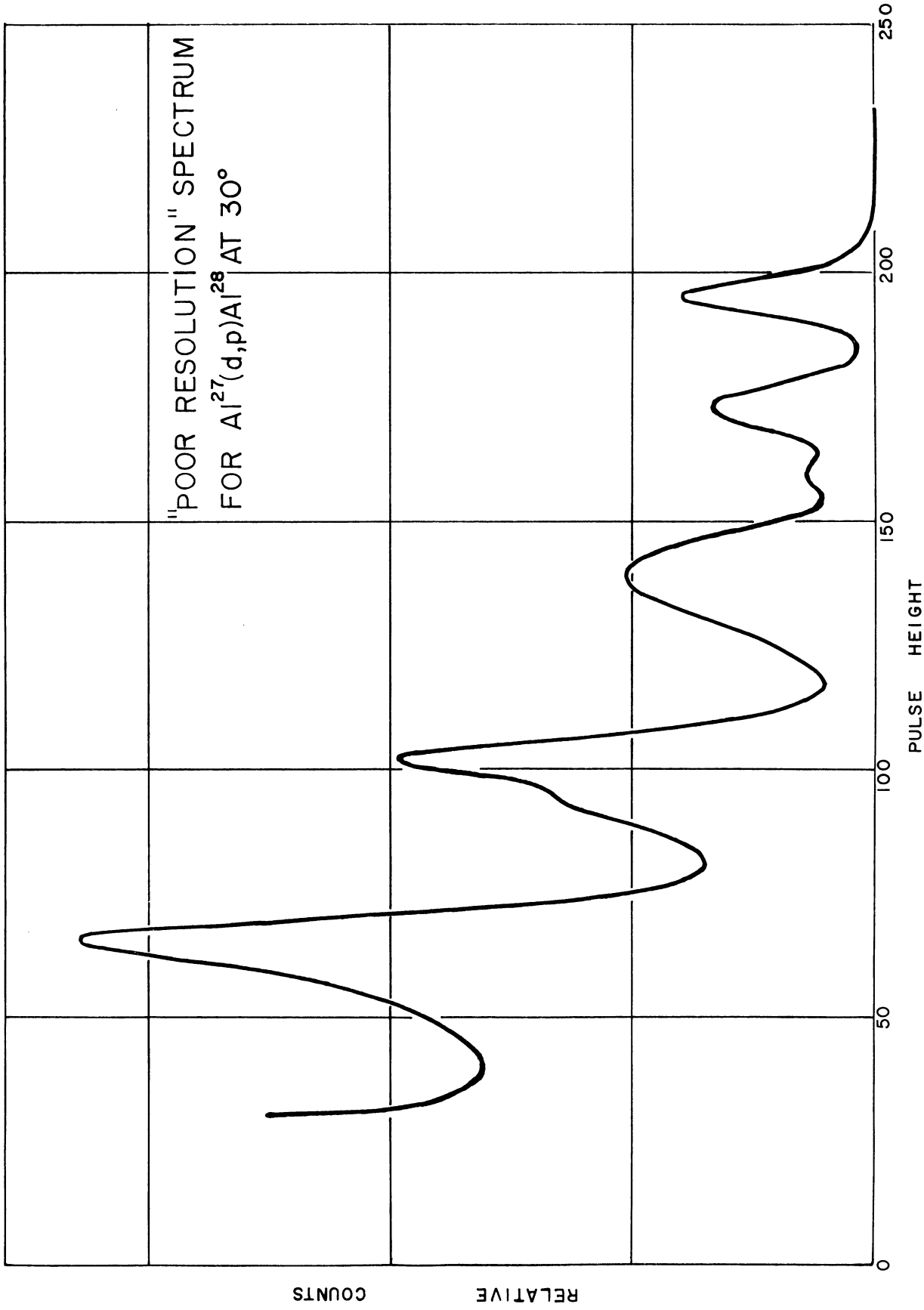
"POOR RESOLUTION" SPECTRUM
FOR $Al^{27}(d,p)Al^{28}$ AT 30°
RELATIVE COUNTS
PULSE HEIGHT
0
50
100
150
200
250

Fig. 20

III. ADDENDUM—PUBLICATION REPRINTS

Reprints not previously submitted of two publications resulting from research under this contract are attached.

These are:

(1) $B^{10}(d,p)B^{11}$ Reaction and the Configurations of B^{11}, O. M. Bilaniuk and J. C. Hensel; Phys. Rev. 120, 211 (1960).

(2) $Ti^{46,48}(d,p)$ $Ti^{47,49}$ Reactions and the $1f_{7/2}^{n}$ and $1f_{7/2}^{n-1}$ Configurations, L. H. Th. Rietjens, O. M. Bilaniuk, and M. H. Macfarlane; Phys. Rev. 120, 527 (1960).